

**Dual control of pcdh8l/PCNS expression and function in *Xenopus laevis* Neural crest cells by adam13/33 via the transcription factors tfap2 $\alpha$  and arid3a.**

Vikram Khedgikar, Genevieve Abbruzzese\*, Ketan Mathavan<sup>2</sup>, Hannah Szydlo, H  l  ne Cousin and Dominique Alfandari<sup>#</sup>.

Department of Veterinary and Animal Sciences, University of Massachusetts Amherst  
MA 01003.

\* David H. Koch Institute for Integrative Cancer Research, Massachusetts Institute of Technology, Cambridge, MA 02139

<sup>2</sup> Molecular and Cellular Biology graduate program. MCB, University of Massachusetts  
Amherst MA 01003

<sup>#</sup>Corresponding author and lead contact: [alfandar@vasci.umass.edu](mailto:alfandar@vasci.umass.edu)

### Abstract:

Adam13/33 is a cell surface metalloprotease critical for cranial neural crest (CNC) cell migration. It can cleave multiple substrates including itself, fibronectin, ephrinB, cadherin-11, pdh8 and pcdh8l (this work). Cleavage of cadherin-11 produces an extracellular fragment that promotes CNC migration. In addition the adam13 cytoplasmic domain is cleaved by gamma secretase, translocates into the nucleus and regulates multiple genes. Here we show that adam13 interacts with the arid3a/drill1/Bright transcription factor. This interaction promotes a proteolytic cleavage of arid3a and its

translocation to the nucleus where it regulates another transcription factor: tfap2 $\alpha$ . Tfap2 $\alpha$  in turn activates multiple genes including the protocadherin pcdh8l (PCNS). The proteolytic activity of adam13 is critical for the release of arid3a from the plasma membrane while the cytoplasmic domain appears critical for the cleavage of arid3a. In addition to this transcriptional control of pcdh8l, adam13 cleaves pcdh8l generating an extracellular fragment that also regulates cell migration.

## **KEYWORDS**

Neural crest; ADAM; Metalloprotease; Disintegrin; cadherin; Protocadherin; Cell Migration; Xenopus; Embryo; tfap2 $\alpha$ ; arid3a; BRIGHT; Drill1; pcdh8l.

## **INTRODUCTION:**

Cranial neural crest (CNC) cells are a transient population of natural stem cells that are induced at the border of the neural and non-neural ectoderm by a combination of signals including BMP, Wnt and FGF (1-3). These signals mediate the expression of key transcription factors that define placodal and neural crest cells (4, 5). Among those the transcription factor tfap2 $\alpha$  is one of the earliest and most conserved factors that controls the fate of neural border cells and later neural crest cells (6, 7). While loss of tfap2 $\alpha$  in all vertebrates tested leads to craniofacial defects, mutations in the tfap2 $\alpha$  gene in humans are associated with the Branchiooculofacial Syndrome highlighting the importance of this

gene for craniofacial development and neural crest cell biology throughout evolution (8-12).

Once induced, CNC cells migrate toward the ventral side of the embryo to contribute to most of the craniofacial structures. Many proteins have been shown to contribute to CNC migration, including multiple cell adhesion molecules such as integrins, cadherins and protocadherins, as well as cell surface metalloproteases that can effectively modulate these adhesion molecules (13). In particular, while cadherin-11 is required at the surface of CNC, an excess of the protein prevents migration (14). The cytoplasmic domain of cadherin-11 binds to the GEF trio and promotes filopodia formation in the migrating CNC (15). In addition, cadherin-11 also localizes to nascent focal adhesion and interacts with the proteoglycan syndecan-4 via its transmembrane domain (16). Lastly, the extracellular domain of cadherin-11 is cleaved by the metalloprotease adam13 producing an extracellular fragment that promotes cell migration (17). This fragment can compete with the integral cadherin-11 to decrease contact inhibition of locomotion by a homophilic dependent binding site, but this site is not required for its ability to promote CNC migration (18).

Other cadherin superfamily members are cleaved by ADAM metalloproteases. In *Xenopus*, the protocadherin pcdh81 is essential for CNC migration both *in vivo* and *in vitro* suggesting that it affects the basic cell locomotion machinery (19). Interestingly, the protocadherin pcdh8 (PAPC), which can functionally replace pcdh81 in the neural crest cells (20) has been shown to be a substrate for adam13 (21). In chick, cleavage of cadherin-6 by adam10 and adam19 is also critical for proper migration of the neural crest cells (22). Thus, controlled expression of cadherin and protocadherin combined with

64 proteolytic processing of these cell adhesion molecules appears to play a critical role in  
65 neural crest cell migration.

66 In addition to its proteolytic cleavage of cadherin-11, adam13/33 has been shown  
67 to play critical roles in CNC induction in *Xenopus tropicalis* by cleaving ephrinB,  
68 reducing its inhibitory activity upon the Wnt signaling pathway and allowing for a robust  
69 expression of *snai2* (23). In contrast, knock down of adam13 in *Xenopus laevis* has no  
70 effect on *snai2* expression but affects CNC migration *in vivo* (24-26). While the  
71 proteolytic role of adam13 is clearly important, the role of its cytoplasmic domain is also  
72 critical. We have shown that the cytoplasmic domain of adam13 is cleaved by gamma  
73 secretase and translocates into the nucleus where it regulates the expression of thousands  
74 of genes. The cleavage by gamma secretase requires a self-proteolytic cleavage by  
75 adam13 in its own cysteine rich domain and is therefore dependent on the adam13  
76 proteolytic activity. In the absence of the cytoplasmic domain, adam13 cannot support  
77 CNC migration, but addition of a soluble form of its cytoplasmic domain fused to GFP,  
78 which partition exclusively in the nucleus, rescues cell migration. Similarly, addition of a  
79 single Leucine in the cytoplasmic domain of adam13 that creates a nuclear export signal  
80 prevents adam13 ability to rescue CNC migration. This ability to regulate cell migration  
81 and gene expression is shared by the cytoplasmic domains of adam13 orthologues from  
82 *C-elegans* to marsupial, as well as the cytoplasmic domains of adam19 from frog and  
83 mouse, demonstrating the evolutionary conservation of this role. In contrast, the  
84 cytoplasmic domains of adam9 and adam10, which also translocate into the nucleus,  
85 cannot compensate for the loss of the adam13 cytoplasmic domain, revealing the  
86 specificity of this activity (24).



Because, the cytoplasmic domain of adam13 does not possess any sequence similarity with transcription factors we have investigated how it can modulate the expression of so many target genes. Here we show that adam13 regulates the expression of the transcription factor tfap2 $\alpha$ , which in turns regulates the protocadherin pcdh8l, a target of adam13 critical for CNC migration. We further show that adam13 physically interacts with the transcription factor arid3a/drill1/BRIGHT. This transcription factor is required for adam13's ability to induce tfap2 $\alpha$ . In human Hek293T cells, adam13 stimulates the production of a shorter fragment of arid3a at the plasma membrane, which translocates to the nucleus. The production of the shorter fragment depends on the adam13 cytoplasmic domain, while the translocation from the membrane depends on the adam13 proteolytic activity. We propose that adam13 may interact with arid3a at the plasma membrane providing a pool of transcription factor that can be released upon cleavage of the adam13 cytoplasmic domain. This function is likely conserved and could contribute to many of the biological processes that are regulated by ADAM proteins (27-32).

## **RESULTS:**

### **Adam13 cleaves pcdh8l**

We have previously shown that adam13 cleaves the protocadherin pcdh8 (21). Given the similarity in sequence between pcdh8 and pcdh8l and the critical role that pcdh8l plays during CNC migration, we hypothesized that adam13 may also cleave pcdh8l. To test this hypothesis, we co-transfected an N-terminal flag-tagged-pcdh8l (Figure 1A) along with

either adam13 (A13) or a proteolytically inactive mutant form adam13E/A (A13E/A) in human Hek293T cells. Western blot analysis of conditioned media from transfected cells shows the presence of the extracellular fragment of pcdh8l only when co-transfected with adam13 (Figure 1B). The approximate size of the fragment (>60 kDa) suggests that it includes the cadherin repeats 1 to 4 of pcdh8l (EC1-4). This was confirmed by generating a truncated form of pcdh8l including these domains, which migrates at the same position as the cleaved fragment (data not shown). No fragment was observed when pcdh8l was co-transfected with A13E/A suggesting that the proteolytic activity of adam13 is responsible for the cleavage of pcdh8l. To confirm these finding *in vivo*, we generated a monoclonal antibody to the cytoplasmic domain of pcdh8l (mAb 2F4). This antibody recognizes a protein of the appropriate size (120 kDa), expressed at the appropriate stage (stage 20), localized to the CNC in whole mount immunostaining and to the plasma membrane of CNC cells *in vitro*. We further confirmed that it recognizes pcdh8l but not pcdh8 transfected in Hek293T cells (Figure 1: figure supplement 1). At stage 20, the main protein recognized is the full length at 120 kDa, but two minor shorter fragments can be seen at  $\approx 60$  (1) and  $\approx 40$  kDa (2) respectively (Figure 1: figure supplement 2). These fragments increased in embryos injected with the adam13 mRNA suggesting that adam13 can also cleave pcdh8l *in vivo*.

### **The pcdh8l fragment can partially compensate for the loss of adam13**

Adam13 cleaves cadherin-11 to generate a fragment that promotes CNC migration (17, 18, 24). To test if the extracellular fragment of pcdh8l also regulates CNC migration we

attempted to rescue the CNC migration defect induced by the loss of adam13 by expressing various forms of pcdh8l. To that effect, we injected an antisense Morpholino oligonucleotide known to block adam13 translation (MO13) (17) at the one-cell stage and the various mRNA at the 8-cell-stage in a dorsal animal blastomere (33). A lineage tracer (RFP mRNA) was co-injected in all cases to follow the migration of the CNC as previously described (17, 18, 21, 24, 26). When MO13 is injected alone 57% of the embryos show no fluorescent CNC in the migration pathways (Figure 1C-D). Injection of a MO13-resistant adam13 mRNA significantly rescued CNC migration (26% inhibition). Injection of the pcdh8l extracellular fragment (EC1-4) mRNA rescued CNC migration significantly (47% inhibition), but less efficiently than the adam13 mRNA. Surprisingly, we found that loss of adam13 could be significantly rescued by the full length pcdh8l mRNA even more efficiently (36% inhibition) than with EC1-4, a phenomenon that was not observed for cadherin-11 (17). These results suggest that the loss of adam13 does not simply prevent the cleavage of pcdh8l but could also affect its expression, localization or function.

#### **Adam13 regulates pcdh8l expression**

We first tested if the loss of adam13 affects pcdh8l expression. For this, MO13 (10ng) was injected at the one-cell-stage, embryos were raised until stage 20 when pcdh8l expression is maximal (19), at which time mRNA and protein were extracted for analysis. In these conditions adam13 Knockdown (KD), which reduces the adam13 protein to undetectable levels (Figure 2C, A13 Pro-P and Mature-M) reduced the expression of pcdh8l mRNA by 43% (Figure 2A). To confirm this data, we injected MO13 (5ng) into

one blastomere of two-cell-stage embryos. The embryos were then fixed and stained by *in situ* hybridization with a pcdh8l probe. We observed that at stage 20, 71% of the embryos showed a reduced expression of pcdh8l on the injected side when compared to the non-injected control side (Figure 2B, N=31). We also tested the protein level of pcdh8l by western blot, using mAb 2F4 (Figure 2C). When compared to non-injected embryos, the level of pcdh8l protein was significantly reduced. Because both adam13 and pcdh8l are also expressed in the somites, we tested if the reduction of pcdh8l was detectable in isolated CNC explants. CNC isolated from embryos injected with MO13 had a 36% reduction of pcdh8l mRNA compared to control CNC (Figure 2: figure supplement 1A). Again, western blot analysis with 2F4 showed a similar trend for the pcdh8l protein (Figure 1: figure supplement 1B). These results show that loss of adam13 results in a significant decrease of pcdh8l expression.

To test if adam13 could induce pcdh8l, we injected mRNA encoding either the wild-type adam13 or various mutant forms of the protein at the one-cell stage and dissected the naïve ectoderm (animal cap, AC) at stage 9. The animal cap explants were then grown until the control embryos reached neurula stage (17 to 20) and mRNA and protein expression were assessed by real-time PCR and Western blot respectively. Analysis of mRNA levels show that wild-type adam13 induces pcdh8l expression whereas its catalytically inactive form (A13E/A), a mutant lacking the cytoplasmic domain ( $\Delta$ Cyto) and the isolated cytoplasmic domain (C13) all fail to induce expression of pcdh8l (Figure 3A). These results were confirmed at the level of pcdh8l protein expression using mAb 2F4 (Figure 3B). These results show that adam13 can induce the

expression of pcdh8l in naïve ectoderm and that both the proteolytic activity and the cytoplasmic domain are required for this function.

### **Adam13 regulates tfap2 $\alpha$ expression**

We have previously shown that adam13 can regulate multiple genes including the cytoplasmic protease Capn8a (24). While we showed that the cytoplasmic domain of adam13 is cleaved and translocates into the nucleus, there are no known DNA binding motifs or transactivation domains in its sequence. For this reason we tested whether adam13 could regulate the expression of a transcription factor known to activate the expression of Cpn8a and pcdh8l. Tfap2 $\alpha$  is such a transcription factor and it plays a key role in neural plate border specification where adam13 is expressed prior to neural crest migration (7, 34, 35). As described above for pcdh8l, we used the Morpholino to adam13 to inhibit adam13 translation in embryos and collected them at stage 20. The real-time PCR data indicate that MO13 reduces tfap2 $\alpha$  mRNA expression to 67% of control embryos (Figure 4A). *In situ* hybridization with a tfap2 $\alpha$  probe shows that loss of adam13 reduces tfap2 $\alpha$  mRNA expression on the injected side in 76% of the embryos (Figure 4B). To test if adam13 could regulate the tfap2 $\alpha$  promoter, we cloned 2.5 Kbp of the *Xenopus laevis* genomic sequence upstream of the transcription start of the tfap2 $\alpha$  gene into a luciferase vector (pGlo3, Bio-rad). We then injected at the 8-cell-stage in the dorsal animal blastomere the tfap2 $\alpha$ :luciferase plasmid together with a Renilla control plasmid in both control embryos and embryos lacking adam13. Analysis of the luciferase activity in dissected CNC explants shows a significant reduction of the tfap2 $\alpha$  promoter

activity following adam13 KD (Figure 4C). This decrease is nearly identical to the observed reduction of the endogenous tfap2 $\alpha$  mRNA (Figure 4A) suggesting that this reporter contains the key responsive elements regulated by adam13.

## **The adam13 cytoplasmic domain is critical for tfap2 $\alpha$ induction**

Given that adam13 is required for proper tfap2 $\alpha$  expression, we then tested if adam13 expression in naïve ectoderm could induce tfap2 $\alpha$  expression. Again we injected embryos at the one cell-stage with the various constructs. Animal caps were dissected at the blastula stage and cultured until sibling embryos reached neurula stage (17 to 20) to isolate mRNA for real-time PCR. The results show that compared to non-injected control (NI), animal caps injected with adam13 RNA have a significant increase in tfap2 $\alpha$  mRNA expression levels (Figure 5A). Similar to what was observed for pcdh8l, both the cytoplasmic domain and the proteolytic activity of adam13 are required for the full expression of tfap2 $\alpha$ .

We then used the tfap2 $\alpha$ :luciferase construct to test if adam13 could induce tfap2 $\alpha$  expression in Human Hek293T cells. As seen in figure 5B, transfection of adam13 results in an almost 4-fold increase in tfap2 $\alpha$  promoter activity. We previously showed that the cytoplasmic domains of adam13 and 19 could rescue CNC migration in embryos expressing adam13 lacking a cytoplasmic domain ( $\Delta$ Cyto), while the cytoplasmic domain of adam9 could not. In addition both adam13 and 19 cytoplasmic domains could rescue the expression of Cpn8a in CNC while adam9 could not (24). We

therefore tested the ability of adam9, 13 and 19 to induce the tfap2 $\alpha$  promoter (Figure 5B). As expected, only adam13 and adam19 could induce the expression of tfap2 $\alpha$  while adam9 could not. In addition, the cytoplasmic domain of adam13 was critical for tfap2 $\alpha$  induction. As seen for pcdh8l, the cytoplasmic domain alone was not able to induce tfap2 $\alpha$  expression. In contrast to what was seen in the animal cap, the proteolytically inactive adam13 (A13E/A) mutant was able to induce the reporter even if less efficiently than the wild type adam13.

#### **Adam13 regulation of pcdh8l depends on tfap2 $\alpha$**

To test if tfap2 $\alpha$  was involved in adam13 induction of pcdh8l, we expressed adam13 in animal cap with or without knocking down tfap2 $\alpha$ . As seen before, injection of adam13 results in an increase in expression of pcdh8l and tfap2 $\alpha$  mRNA (Figure 5C and D). In contrast, injection of a tfap2 $\alpha$  morpholino prevented the induction of both pcdh8l and tfap2 $\alpha$  by adam13 (Figure 5C and D). In *Xenopus tropicalis*, adam13 has been shown to positively regulate the Wnt signaling pathway (23) and Wnt/ $\beta$ -catenin has been shown to regulate tfap2 $\alpha$ . To test if adam13 control of pcdh8l or tfap2 $\alpha$  also involves this pathway we injected embryos with a morpholino to  $\beta$ -catenin (36). The results show that reduction of  $\beta$ -catenin does not prevent adam13 induction of pcdh8l or tfap2 $\alpha$  (Figure 5C and 5D). Interestingly adam13 up-regulation of tfap2 $\alpha$  was also inhibited by the morpholino to tfap2 $\alpha$  suggesting a positive feedback loop mechanism in which, tfap2 $\alpha$  is involved in its own regulation by adam13 (Figure 5D).

240

241 **Adam13 physically interacts with arid3a and FoxD3.**

242 Our results suggest that adam13 can directly regulate the tfap2 $\alpha$  promoter. However,  
243 there is no evidence that the cytoplasmic domain of adam13 can interact with DNA. In  
244 addition, fusing the adam13 cytoplasmic domain with the VP-16 trans-activator domain  
245 does not induce the expression of tfap2 $\alpha$  (Alfandari, unpublished result). Taken together,  
246 these results suggest that adam13 may interact with and regulate a transcription factor  
247 that controls tfap2 $\alpha$  expression. To test this hypothesis we narrow down the list of  
248 potential candidate transcription factors based on the presence of their binding site on the  
249 tfap2 $\alpha$  promoter (Jaspar (37)), their expression in the CNC (Xenbase, (38, 39)), and their  
250 ability to induce the tfap2 $\alpha$  luciferase reporter in Hek293T cells (data not shown). We  
251 then tested whether any of these transcription factors could physically interact with  
252 adam13. Two transcription factors (foxd3 and arid3a) were positive in all assays and  
253 were tested for adam13 binding by co-immunoprecipitation (Figure 6). When injected in  
254 embryos, arid3a-flag co precipitated with adam13 (Figure 6A). This interaction was lost  
255 when adam13 was KD (MO13). Similarly when foxd3-myc RNA was injected in  
256 embryos either alone or with the adam13 MO, the foxd3 protein was co-precipitated with  
257 the endogenous adam13 protein and was absent when adam13 was KD (Figure 6B).  
258 These results show that both transcription factors can interact with adam13 *in vivo*.

259

260 **Arid3a is critical for tfap2 $\alpha$  and pcdh8l expression.**



We then tested whether *foxd3* and *arid3a* were required for *adam13* induction of *tfap2α* and *pcdh8l* using the animal cap assay (Figure 7A-B). The real-time PCR shows that while *arid3a* KD efficiently prevented *adam13* induction of both *tfap2α* and *pcdh8l*, *foxd3* KD had no effect. In these experiments, loss or gain of *adam13* function had no effect on *arid3a* and *foxd3* expression (Figure 7 – Figure supplement 1).

Because *arid3a* was shown to regulate TGFβ signaling downstream of Smad2 (40) and the ability of mammalian ADAM12 to mediate TGFβ signaling (41), we investigated whether *adam13* induction of *pcdh8l* and *tfap2α* requires Smad2. Animal cap experiments show that *adam13* induces *tfap2α* and *pcdh8l* expression even when Smad2 is knocked down (Figure 8A-B). In addition Smad2 does not induce the *tfap2α* promoter in Hek293T cells and the inhibitory Smad, Smad7 does not prevent *adam13* induction of the *tfap2α* promoter in the same cells (Figure 8C). These results suggest that *adam13* regulation of *tfap2α* does not involve the TGFβ signaling pathway.

While *arid3a* has been shown to be essential for mesoderm specification (40), there is no evidence concerning its role in neural crest cell induction or patterning. Published expression pattern show that it is expressed in the non-neural ectoderm and the neural plate border (40) where it overlaps with *adam13* suggesting that it could play a role in neural crest specification. We therefore investigated the effect of the loss of *arid3a* on the expression of *tfap2α*, *pcdh8l* and the neural crest marker *snai2*. To avoid a general defect in mesoderm patterning, we injected embryos at the 8-cell stage in a single dorsal animal blastomere and tested the expression of the selected genes by *in situ* hybridization

(Figure 9A-C). The results show that loss of arid3a decreased the expression of tfap2 $\alpha$  and pcdh8l as expected but also snai2, suggesting a key role in neural crest cell patterning.

### **Tfap2 $\alpha$ but not arid3a can rescue CNC migration in embryos lacking adam13.**

It is clear that adam13 regulates tfap2 $\alpha$  expression and therefore it is expected that restoring the level of tfap2 $\alpha$  in embryos lacking adam13 should at least partially rescue CNC migration. Indeed, injection of tfap2 $\alpha$  in embryos lacking adam13 significantly rescued CNC migration (Figure 9E-F) in a way similar to that of pcdh8l expression. In contrast expression of arid3a had no effect on CNC migration in embryos lacking adam13. These results are consistent with a model where adam13 requires arid3a to function in the CNC. The facts that arid3a expression is not regulated by adam13 (Figure 7 supplement 1), that both proteins interact (Figure 6) and that arid3a cannot compensate for the loss of adam13 (Figure 9E) suggest that arid3a is not downstream of adam13 but rather that the two proteins work together.

### **Adam13 stimulates Arid3a nuclear translocation**

To test if adam13 could regulate Arid3a translocation to the nucleus, we performed nuclear and cytoplasmic fractionation of transfected Hek293T cells (Figure 10). As expected we found that arid3a is equally distributed between the cytoplasmic and nuclear compartment (Figure 10A). Interestingly, in the nucleus a smaller fragment (40 kDa) is observed, and this fragment is much more abundant in the nucleus of cells co-transfected

with adam13. We then tested if this fragment was also observed in cells co-transfected with the adam13 protease dead mutant (A13E/A) and the mutant lacking the cytoplasmic domain (A13ΔCyto). In both conditions we found that the fragment was not increased by these mutants (Figure 10B). We then tested if Arid3a was localized to the plasma membrane in Hek293T cells, as previously described for B-cells, and if adam13 and the various mutants affected this localization (Figure 10C). Transfected Arid3a was found in the membrane fraction of Hek293T cells in all conditions tested. In cells expressing adam13, the 40 kDa fragment of arid3a (arid3a Short) was enriched. This fragment was dramatically increased in cells expressing the A13E/A mutant, suggesting that the proteolytic activity of adam13 is not responsible for the production of arid3a Short. In contrast, cells expressing A13ΔCyto express the same level of arid3a Short than those expressing only arid3a. Taken together, these results show that adam13 regulates arid3a post-translational modification (proteolytic cleavage) and nuclear translocation. These results are compatible with a model (Figure 11) in which the adam13 cytoplasmic domain is part of a complex that either cleaves arid3a at the plasma membrane or stabilizes a cleaved form of arid3a (Figure 11-1). Upon adam13 self-proteolysis (24, 42) (Figure 11-2), gamma secretase can cleave the cytoplasmic domain of adam13 (Figure 11-3), which then translocates with or without arid3a to the nucleus (Figure 11-4). In the absence of adam13 proteolytic activity the complex remains stable at the plasma membrane (Figure 10C), while in the absence of the cytoplasmic domain the complex is not formed.

## DISCUSSION

Our results show that adam13 expression is essential for the proper expression of tfap2 $\alpha$ , a transcription factor that defines the neural plate border in all vertebrates studied so far (7-10, 12, 43). This regulation is mediated by the interaction of adam13 with the arid3a transcription factor and requires both the cytoplasmic domain and metalloprotease activity of adam13 in naïve ectoderm. Our results suggest that the cytoplasmic domain of adam13 is critical for either stabilizing or inducing the cleavage of arid3a at the plasma membrane. This fragment is then accumulated in the nucleus of cells co-transfected with adam13. The accumulation of this fragment in the nucleus appears to be controlled by the adam13 proteolytic activity, as it is impaired in the A13E/A mutant. Given adam13's ability to cleave itself within its cysteine rich domain (42), thus becoming a substrate for gamma-secretase, to cleave and release the cytoplasmic domain from the membrane (24), we propose that the complex containing the cleaved arid3a, and at least the adam13 cytoplasmic domain is then free to translocate into the nucleus (Figure 11). This model is consistent with the essential roles of both the proteolytic and cytoplasmic domain of adam13 in animal cap and the CNC. It is also consistent with the observation that the GFP-C13 fusion protein containing the adam13 cytoplasmic domain, which is only found in the nucleus is unable to induce tfap2 $\alpha$  expression. On the other hand, the fact that the adam13 E/A mutant can induce the reporter in Hek293T cells even at a lower efficiency is puzzling. While this construct clearly increases the arid3a fragment, it does not allow its efficient nuclear translocation (Figure 10B and C). One possible explanation is that it may act as a dominant mutant by trapping e2f1 at the plasma membrane. Arid3a was originally identified in a screen of E2F1 binding protein as E2FBP1 (44). In Hek293T cells, e2f1 inhibits the tfap2a promoter activity and is able to block both adam13 and

arid3a induction of the reporter (data not shown). Thus by binding to the endogenous E2F1 protein in Hek293T cells, A13E/A could sequester E2F1 at the plasma membrane and increase the reporter activity. In *Xenopus*, e2f1 is expressed maternally and is strongly down regulated at stage 20 (45) when the animal caps are extracted. Thus A13E/A expression would have no effect on its ability to translocate in the nucleus.

In B-cells, ARID3a also known as Bright, is post translationally modified. First, it is palmitoylated and associate with lipid raft at the plasma membrane (46). Upon stimulation of the B-cell receptor, arid3a is sumoylated, dissociate from the lipid raft and is then free to regulate gene expression (47). It is possible that in the neural crest cells, adam13 regulates a pool of arid3a associated with lipid raft at the plasma membrane. It could do this by helping assemble the proper signaling complex including the enzyme responsible for arid3a post-translational modification. In the complex the presence of a protease would cleave off the N-terminal domain of arid3a. This cleavage could be important for releasing a transcriptional inhibitor (e.g. e2f1) or simply destabilizing arid3a interaction with the plasma membrane. Given the widespread expression of arid3a, this would provide a mechanism by which the transcription factor is only activated in the right cells and at the right time. Our results show that adam13 expression dramatically increases the nuclear localization of a cleavage product of arid3a (arid3a Short), while it does not affect the overall distribution of the intact arid3a protein. This depends on both the proteolytic activity and the cytoplasmic domain of adam13. It is tempting to speculate that this fragment (arid3a Short), which has not been describe before, is responsible for the increased expression of tfap2 $\alpha$ . Based on the calculated molecular weight of the fragment it is likely to maintain the intact ARID (DNA binding) domain as well as the

RECKLES domain that control the nuclear localization. It will be interesting to determine if adam13 stabilize arid3a Short or produces it. If this model were correct we would expect that proteins that interfere with the production of the cleaved cytoplasmic domain would also interfere with adam13's ability to induce tfap2 $\alpha$ . We have previously shown that the secreted Wnt receptor Fz4-v1, binds to adam13 and prevents its proteolytic activity. We further showed that KD of Fz4-v1 induces an early production of the adam13 cytoplasmic fragment (48). In embryos, KD of Fz4-v1, increases both tfap2 $\alpha$  and pcdh8l transcription (data not shown), while In Hek293T cells, expression of Fzd4-v1 inhibits adam13 activation of the tfap2 $\alpha$  reporter further supporting our model.

Our results also show that adam13 activation of tfap2 $\alpha$  in naïve ectoderm does not require  $\beta$ -catenin, while tfap2 $\alpha$  has been shown to be induced by  $\beta$ -catenin in the CNC (7). In addition, we also show that adam13 induction of tfap2 $\alpha$  requires the presence of tfap2 $\alpha$ . Both adam13 and tfap2 $\alpha$  are initially expressed in the entire ectoderm and become excluded from the neural plate to be restricted to the neural folds and later neural crest (35, 49). In addition, the quantitative expression pattern of tfap2 $\alpha$  and adam13 by RNA-seq is nearly identical (45). This suggests that adam13 and tfap2 $\alpha$  expression is initially controlled by the same transcription factor possibly  $\beta$ -catenin (50), and that adam13 is later required for the maintenance and amplification of tfap2 $\alpha$  expression within the neural fold and neural crest cells. This is compatible with the fact that adam13 is not required for  $\beta$ -catenin induction of snai2 in the CNC in *Xenopus laevis*. Also consistent with this model, we find that both arid3a and tfap2 $\alpha$  can induce the tfap2 $\alpha$  reporter individually and the combination of these two proteins

393 produces an additive increase in the luciferase expression (data not shown). We also  
394 tested if adam13 could initiate a full CNC program in naïve ectoderm. We found that  
395 while snail2 and twist can be induced by adam13, cadherin 11, sox8 and sox10 were not  
396 (data not shown) suggesting that adam13 is not capable to induce neural crest cells from  
397 naïve ectoderm.

398       Ultimately adam13 induction of tfap2 $\alpha$  results in the induction of pcdh8l and the  
399 up-regulation of Cpn8a in the CNC, two proteins critical for CNC migration. The fact  
400 that CNC lacking adam13 can migrate *in vitro* while those missing pcdh8l cannot (19)  
401 might be explained by the observation that the CNC lacking adam13 eventually express  
402 both tfap2 $\alpha$  and pcdh8l suggesting that another control of tfap2 $\alpha$  expression is activated  
403 later on. This may or may not require the involvement of other ADAM proteases. In  
404 particular, it is possible that adam19, which can activate the tfap2 $\alpha$  reporter in Hek293T  
405 cells may compensate for the loss of adam13 in the CNC. It will be of interest to test if  
406 tfap2 $\alpha$  expression in mouse is also regulated by ADAM proteases and if this contributes  
407 to craniofacial development. Given the conserved ability of the adam19 cytoplasmic  
408 domain from mouse and *Xenopus* to functionally replace the adam13 cytoplasmic  
409 domain, together with the ability of adam19 to induce the tfap2 $\alpha$  reporter, it is tempting  
410 to speculate that adam19, which is expressed in mouse CNC and contributes to the  
411 cardiac neural crest cell development, could regulate tfap2 $\alpha$  to promote CNC migration.  
412 While a role for adam13/33 and adam19 in mouse CNC has not been shown, it is possible  
413 that the craniofacial phenotypes are subtle and may have been missed in the individual  
414 Knock out reports.

Our results show that the extracellular fragment of multiple cadherins and protocadherin can rescue CNC migration. In particular we have shown that the extracellular fragment of Cadherin-11 can rescue CNC migration in embryos lacking adam13 or expressing a non-cleavable form of cadherin-11 (18). Similarly the extracellular fragment of pcdh8l partially rescues CNC migration in embryos lacking adam13. It is interesting to note that one can greatly improve the rescue either by injecting full-length pcdh8l together with adam13 lacking a cytoplasmic domain (data not shown). This mutant form of adam13 can cleave pcdh8l but cannot regulate transcription and therefore the level of the protocadherin. Alternatively, greater rescue is also achieved by expressing the EC1-4 fragment of pcdh8l together with tfap2 $\alpha$  showing that the transcriptional and proteolytic activity of adam13 can be uncoupled. Why can the various cadherin and protocadherin fragments rescue migration? We have shown that the extracellular fragment of cadherin-11 bind to ErbB2 (EGF receptor 2) and regulates Akt phosphorylation (Mathavan et al., submitted). In cancer cells, the extracellular fragment of E-cadherin can also bind to ErbB2 to promote cell migration (51, 52). This suggests that a common structure within the Cadherin/protocadherin extracellular domain can bind and signal through growth factor receptors.

### **The larger role of ADAM regulation of transcription.**

Our results show how ADAMs can regulate transcription via their cytoplasmic domain. Multiple reports have shown ADAM protein in the nuclei (24, 53, 54). Our previous study has shown that most ADAM cytoplasmic domains can translocate into the nucleus



if cleaved from the plasma membrane. For adam13 we have identified a physical interaction with importin  $\beta$ 1, which is known to mediate transport of proteins that do not harbor a canonical nuclear localization signal (Alfandari ms/ms unpublished). Given the essential and conserved role of tfap2 $\alpha$  in craniofacial development (7-12, 55), as well as its ability to reduce the proliferation and migration of multiple cancer cells including those derived from neural crest cells (56-59), it will be essential to study the potential regulation of tfap2 $\alpha$  by human ADAM proteins. Our preliminary results show that mouse adam33 and adam12 are also able to induce the tfap2 $\alpha$  reporter when transfected in Hek293T cells even if less efficiently than adam13 or adam19 while *Xenopus* adam9, 10 and 11 do not (data not shown). A better understanding of the precise regulation of tfap2 $\alpha$  transcription by the various ADAMs will be necessary to determine if they all regulate gene expression by a common mechanism. Similarly, the observed role of adam12 in mediating TGF- $\beta$  signaling, may involve an interaction with arid3a, a protein known to be downstream of the TGF- $\beta$  effector Smad2 (40). The fact that both adam12 and arid3a are critical for trophoblast formation (60-63) suggests that this functional interaction may be important in multiple cell types to mediate key developmental processes.

#### **COMPETING INTERESTS**

The authors have no competing interests.

## **MATERIALS AND METHODS**

### **Antibodies:**

The monoclonal antibody to pcdh8l (mAb2F4) was generated against a bacterial fusion protein corresponding to the entire cytoplasmic domain of pcdh8l using standard hybridoma techniques. It recognizes the endogenous protein by western blot and immunofluorescence. 2F4 does not recognize overexpressed protocadherin pcdh8 and pcdh1. The monoclonal antibody to Rpn1 (Mono5) was generated by immunizing BalbC mice with *Xenopus* XTC cells (64). Hybridomas were screened by ELISA on fixed *Xenopus* XTC cells (RRID:CVCL\_5610) and western blot from embryo extracts. Mono5 was further characterized by shot-gun LC/ms/ms of protein immunoprecipitated using Mono5 from embryo extracts. The identity was confirmed by detecting the recombinant *Xenopus* Rpn1 transfected in Hek293T cells (ATCC®, CRL-3216 RCB2202). All cell lines were treated with mycoplasma removal agent (MRA, MP-Biomedicals) prior to use. The antibody works by western blot and immunofluorescence on the endogenous *Xenopus* protein. The antibodies to adam13 have been described before. 6615F, rabbit polyclonal antibody (35), DC13, Rabbit polyclonal antibody (42), gA13, goat polyclonal antibody to the adam13 cytoplasmic domain (24) mAb 4A7, mouse monoclonal antibody to the cytoplasmic domain of adam13 (21). M2, mouse monoclonal antibody to Flag (Sigma, RRID:AB\_439685). Rabbit polyclonal antibody to tfap2 $\alpha$  (LS-C624, LifeSpan BioSciences, RRID:AB\_2199419).

### **Morpholinos and DNA constructs**

Morpholino antisense oligonucleotides (Gene Tools, Philomath OR) were described elsewhere. MO13 (17), MOtfap2 $\alpha$  (9), MO FoxD3 (65), MO arid3a (40), MOpcdh8l (19), 2006), MOSmad2 (66), MO $\beta$ -catenin (36). Full length pcdh8l and tfap2 $\alpha$  in pCS2 were a generous gift from Dr. Thomas Sargent (NIH, Bethesda, MD, USA). The N-terminal flag tag was added in pcdh8l using the In-Fusion kit (Clontech, CA) according to manufacturer's instruction. The EC1-4 construct was produced by inserting a stop codon in the N-terminus tagged pcdh8l after the fourth cadherin repeat. All ADAM constructs are in pCS2 and have been described before. adam9 (17, 67). adam13, E/A-adam13, A13 $\Delta$ Cyto, GFP-C13 (24, 25), adam19 (68). Monomeric red fluorescent protein (mRFP) in pCS2 was a generous gift from Dr. Jim Smith (Gurdon Institute, Cambridge, United Kingdom). All constructs were sequenced and transfected in Hek293T cells to verify the protein translation, size and surface expression when appropriate.

## **Injectons**

Capped mRNAs were synthesized using SP6 RNA polymerase on DNA linearized with NotI as described before (69). Injectors were calibrated using a 1 $\mu$ l capillary needle (Microcaps, Drumond, PA, USA). The injection pressure was set at 15 psi and the injection time set between 50 and 200ms to obtain a 5nl delivery. For the CNC migration assays, the morpholino was injected at the 1-cell stage and mRNAs at 8-cell stage as described previously (21). Embryos were raised at 15°C until tail bud stage (St. 24 to 28) at which time CNC migration was scored for the presence or absence of fluorescent CNC cells in the migration pathways. For each injection the percentage of inhibition was normalized to embryos injected with RFP alone and set to 0% inhibition. All experiments

were performed at least 3 times using different females to determine statistical significance. Each experiment always included a positive control (RFP) and MO13 in addition to all experimental conditions.

#### **Cell culture and transfection**

Hek293T (ATCC®, CRL-3216 RCB2202) cells were cultured in RPMI media supplemented with Pen/Strep, L-glutamine, sodium pyruvate, and FBS (10 U/ml, 2 mM; 0.11 mg/ml, 10%; Hyclone, South Logan, UT). Transfections were performed using XtremeGENE™ HP DNA Transfection Reagent (Roche, Basel, Switzerland) following the manufacturer's instructions. For pcdh8l shedding assay, cells were incubated with media containing 2% serum for 24 hours after transfection and conditioned media was collected. The shed extracellular domain was purified using Concanavalin-A-agarose (Vector), eluted in reducing Laemmi and blotted using the Flag (M2) monoclonal antibody.

#### **Animal cap dissection**

Embryos were injected at one cell stage with various mRNA constructs or morpholino (quantity provided in figure legends). At stage 9 animal caps were dissected and grown in 0.5X Modified Barth's Saline (1XMBS: 88.0 mM NaCl, 1.0 mM KCl, 2.4 mM NaHCO<sub>3</sub>, 15.0 mM HEPES [pH 7.6], 0.3 mM CaNO<sub>3</sub>-4H<sub>2</sub>O, 0.41 mM CaCl<sub>2</sub>-6H<sub>2</sub>O, 0.82 mM MgSO<sub>4</sub>) with gentamicin (50 µg/ml) on agarose plate at 15°C until control embryos reached stage 17 to 20.

#### **Quantitative PCR**

Quantitative real-time PCR was performed as previously described (68). All primers were tested for efficiency. Embryos and explants were collected at the appropriate stage and

immediately placed in a guanidinium thioisocyanate solution to extract RNA (Roche, RNA isolation Kit). Total RNA was quantified by absorbance at 260 nm using a nanodrop (Thermo Scientific). Polyadenylated RNA was isolated with oligo-dT beads (Qiagen) following manufacturer's instruction. The cDNA was produced using polyA mRNA purified from 10 CNC explants, or 10 animal cap or 5 embryos using direct cDNA synthesis kit (Quanta) according to manufacturer's instruction. Quantitative PCR was performed using SYBR green (Takara, Kyoto, Japan) to measure mRNA levels of *pcdh8l*, *tfap2 $\alpha$*  and *arid3a*. GAPDH was used to normalize total cDNA quantities. Primer sequences are given in Table1. The  $\Delta\Delta CT$  (70) technique was used to calculate fold changes. All results are presented as the fold change compare to non-injected.

**Table 1:**

| Target                   | Sequence 5'-3'           |
|--------------------------|--------------------------|
| xltfap2 $\alpha$ Forward | ATAACAATGCGGTGTCGTCCCTCT |
| xltfap2 $\alpha$ Reverse | AGAGCCTTCTCTGGACTTCTGCAA |
| xlarid3a Forward         | GGAGGCTTGGTGGAAGTTATTA   |
| xlarid3a Reverse         | ACTGAGTGCGCAGAGTAAAG     |
| xlGAPDH Forward          | TTAAGACTGCATCAGAGGGCCCAA |
| xlGAPDH Reverse          | GGGCAATTCCAGCATCAGCATCAA |
| xlpcdh8l Forward         | TCTCAACTCGTGCTCAAATC     |
| xlpcdh8l Reverse         | CCTCTGCTGACCCATTATTC     |

## Immunoprecipitation and Western blots

Hek293T cells, embryos and explants were all extracted in 1XMBS with 1% Triton-X100, protease phosphatase inhibitor cocktail (Thermoscientific) and 5 mM EDTA. Immunoprecipitations were performed using 1-5 µg of antibody bound to ProteinA/G-agarose beads (Thermoscientific) either 2 hours at room temperature or overnight at 4°C. Beads were washed 3 times with the extraction buffer prior to elution with Laemmli buffer. All proteins were separated on 5-22% gradient SDS-PAGE gels and transferred to polyvinylidene fluoride membranes (PVDF, Millipore, Billerica, MA) using a semi-dry transfer apparatus (Hoeffer). pcdh8l Glycoprotein was pulled down from total protein extract with concanavalin-A agarose beads (Vector Laboratories, Burlingame, CA). Cytoplasmic and nuclear extracts were performed using the NEper kit (Pierce) following manufacturer instructions. Purification of total membrane was adapted from (71), Hek293T cells were washed once with PBS and collected by pipetting up and down in ice cold EB (10 mM Hepes pH7.5, 0.3M sucrose, 1mM EDTA). Cells were collected by spinning at 300 g for 5 min and were then extracted using multiple passages through a 25g needle (1 ml for a single well of a 6 well plate) of EB buffer complemented with protease phosphatase inhibitor cocktail (Thermoscientific) and 5 mM EDTA. Intact cells and nuclei were pelleted at 1000g for 10 min at 4°C. The supernatant were spun at 45,000rpm/88,000g (Beckman optima, TLA 100.2) for 30 min at 4°C. The membrane pellet was re-suspended in 100 µl of laemmly buffer. For embryos, 20 embryos were extracted in 500 µl of EB buffer, cell debris and nuclei were spun down at 1,000g at 4°C for 15 min. The supernatant was then spun at 45,000rpm/88,000g at 4C for 30 min to pellet the total membranes.

## **Whole Mount in Situ Hybridization**

Whole mount in situ hybridization was performed using previously described protocol (Harland, 1991). *pcdh8l*, *tfap2 $\alpha$*  and *snai2* probes were generated using diogoxigenin-rUTP-label. Images were taken using a Zeiss stereo microscope Lumar-V12 with the Axiovision software package.

## **Luciferase Activity for *tfap2 $\alpha$* promoter**

Hek293T cells were seeded in 6-well plates at 30% confluence the day before transfection. The total amount of DNA per well was adjusted to 1  $\mu$ g and included 100 ng of the *tfap2 $\alpha$*  promoter:luciferase and 100 pg of pRL-CMV. All plasmids were transfected using X-tremeGENE™ HP as described above. 24 hours after transfection, cells were lysed and processed using the Dual-Luciferase Reporter Assay System protocol (Promega, Madison, WI). For *in vivo* experiments, 100 pg of the *tfap2 $\alpha$* :luciferase promoter and 10 pg of pRL-CMV were injected at the 8 cell stage in a dorsal animal blastomere. Whole embryos or dissected CNC explants were lysed and processed following the Dual-Luciferase Reporter Assay System protocol. The Luminescence Signals were measured using a luminometer microplate reader (BMG LABTECH Ortenberg, Germany).

## **Statistical Methods**

For *in vivo* experiments, each experiment was repeated at least three times on separate days using on average 30 embryos per case per experiment. For Q-PCR and luciferase assays, all experiments were performed at least 3 times (biological repeats) and each PCR was performed in triplicate. Error bars represent standard error to the mean. One-way

ANOVA (non-parametric) was performed using Newman–Keuls to determine statistical significance. Statistically significance was set at \* $p < 0.05$ , \*\* $p < 0.01$  and \*\*\* $p < 0.005$ .

#### AKNOWLEDGEMENT:

This work was supported by the National Institutes of Health, U.S. Public Health Service, Grant RO1-DE016289 to D.A., F31-DE023275 to G.A and RO3-DE025692 to H.C. The author would like to thank Vanessa Bartollo, Hannah Szydlo, Peri Prendergast, Erin Kerdavid, and Brittany Woodland for their contribution to experiments in this manuscript.

#### REFERENCES

1. Dorsky RI, Moon RT, Raible DW. Control of neural crest cell fate by the Wnt signalling pathway. *Nature*. 1998;396(6709):370-3.
2. Monsoro-Burq AH, Fletcher RB, Harland RM. Neural crest induction by paraxial mesoderm in *Xenopus* embryos requires FGF signals. *Development*. 2003;130(14):3111-24.
3. Tribulo C, Aybar MJ, Nguyen VH, Mullins MC, Mayor R. Regulation of *Msx* genes by a Bmp gradient is essential for neural crest specification. *Development*. 2003;130(26):6441-52.
4. Groves AK, LaBonne C. Setting appropriate boundaries: fate, patterning and competence at the neural plate border. *Dev Biol*. 2014;389(1):2-12.
5. Milet C, Monsoro-Burq AH. Neural crest induction at the neural plate border in vertebrates. *Dev Biol*. 2012;366(1):22-33.
6. de Croze N, Maczkowiak F, Monsoro-Burq AH. Reiterative AP2a activity controls sequential steps in the neural crest gene regulatory network. *Proc Natl Acad Sci U S A*. 108(1):155-60.
7. de Croze N, Maczkowiak F, Monsoro-Burq AH. Reiterative AP2a activity controls sequential steps in the neural crest gene regulatory network. *Proc Natl Acad Sci U S A*. 2011;108(1):155-60.
8. Hoffman TL, Javier AL, Campeau SA, Knight RD, Schilling TF. *Tfap2* transcription factors in zebrafish neural crest development and ectodermal evolution. *J Exp Zool B Mol Dev Evol*. 2007;308(5):679-91.
9. Luo T, Lee YH, Saint-Jeannet JP, Sargent TD. Induction of neural crest in *Xenopus* by transcription factor AP2alpha. *Proc Natl Acad Sci U S A*. 2003;100(2):532-7.



10. Martinelli M, Masiero E, Carinci F, Morselli PG, Palmieri A, Girardi A, et al. Evidence of an involvement of TFAP2A gene in non-syndromic cleft lip with or without cleft palate: an Italian study. *Int J Immunopathol Pharmacol*. 2011;24(2 Suppl):7-10.
11. Meshcheryakova TI, Zinchenko RA, Vasilyeva TA, Marakhonov AV, Zhylina SS, Petrova NV, et al. A clinical and molecular analysis of branchio-oculo-facial syndrome patients in Russia revealed new mutations in TFAP2A. *Ann Hum Genet*. 2015;79(2):148-52.
12. Van Otterloo E, Li W, Garnett A, Cattell M, Medeiros DM, Cornell RA. Novel Tfp2-mediated control of soxE expression facilitated the evolutionary emergence of the neural crest. *Development*. 2012;139(4):720-30.
13. Alfandari D, Cousin H, Marsden M. Mechanism of *Xenopus* cranial neural crest cell migration. *Cell Adh Migr*. 2010;4(4):553-60.
14. Borchers A, David R, Wedlich D. *Xenopus* cadherin-11 restrains cranial neural crest migration and influences neural crest specification. *Development*. 2001;128(16):3049-60.
15. Kashef J, Kohler A, Kuriyama S, Alfandari D, Mayor R, Wedlich D. Cadherin-11 regulates protrusive activity in *Xenopus* cranial neural crest cells upstream of Trio and the small GTPases. *Genes Dev*. 2009;23(12):1393-8.
16. Langhe RP, Gudzenko T, Bachmann M, Becker SF, Gonnermann C, Winter C, et al. Cadherin-11 localizes to focal adhesions and promotes cell-substrate adhesion. *Nat Commun*. 2016;7:10909.
17. McCusker C, Cousin H, Neuner R, Alfandari D. Extracellular cleavage of cadherin-11 by ADAM metalloproteases is essential for *Xenopus* cranial neural crest cell migration. *Mol Biol Cell*. 2009;20(1):78-89.
18. Abbruzzese G, Becker SF, Kashef J, Alfandari D. ADAM13 cleavage of cadherin-11 promotes CNC migration independently of the homophilic binding site. *Dev Biol*. 2016;415(2):383-90.
19. Rangarajan J, Luo T, Sargent TD. PCNS: a novel protocadherin required for cranial neural crest migration and somite morphogenesis in *Xenopus*. *Dev Biol*. 2006;295(1):206-18.
20. Schneider M, Huang C, Becker SF, Gradl D, Wedlich D. Protocadherin PAPC is expressed in the CNC and can compensate for the loss of PCNS. *Genesis*. 2014;52(2):120-6.
21. Abbruzzese G, Cousin H, Salicioni AM, Alfandari D. GSK3 and Polo-like kinase regulate ADAM13 function during cranial neural crest cell migration. *Mol Biol Cell*. 2014;25(25):4072-82.
22. Schiffmacher AT, Padmanabhan R, Jhingory S, Taneyhill LA. Cadherin-6B is proteolytically processed during epithelial-to-mesenchymal transitions of the cranial neural crest. *Mol Biol Cell*. 2014;25(1):41-54.
23. Wei S, Xu G, Bridges LC, Williams P, White JM, DeSimone DW. ADAM13 induces cranial neural crest by cleaving class B Ephrins and regulating Wnt signaling. *Dev Cell*. 2010;19(2):345-52.
24. Cousin H, Abbruzzese G, Kerdavid E, Gaultier A, Alfandari D. Translocation of the cytoplasmic domain of ADAM13 to the nucleus is essential for Calpain8-a expression and cranial neural crest cell migration. *Dev Cell*. 2011;20(2):256-63.

25. Alfandari D, Cousin H, Gaultier A, Smith K, White JM, Darribere T, et al. *Xenopus* ADAM 13 is a metalloprotease required for cranial neural crest-cell migration. *Curr Biol*. 2001;11(12):918-30.
26. Cousin H, Abbruzzese G, McCusker C, Alfandari D. ADAM13 function is required in the 3 dimensional context of the embryo during cranial neural crest cell migration in *Xenopus laevis*. *Dev Biol*. 2012;368(2):335-44.
27. Alfandari D, McCusker C, Cousin H. ADAM function in embryogenesis. *Semin Cell Dev Biol*. 2009;20(2):153-63.
28. Drey Mueller D, Pruessmeyer J, Groth E, Ludwig A. The role of ADAM-mediated shedding in vascular biology. *Eur J Cell Biol*. 2012;91(6-7):472-85.
29. Giebeler N, Zigrino P. A Disintegrin and Metalloprotease (ADAM): Historical Overview of Their Functions. *Toxins (Basel)*. 2016;8(4):122.
30. Lu X, Lu D, Scully M, Kakkar V. ADAM proteins - therapeutic potential in cancer. *Curr Cancer Drug Targets*. 2008;8(8):720-32.
31. Pollheimer J, Fock V, Knofler M. Review: the ADAM metalloproteinases - novel regulators of trophoblast invasion? *Placenta*. 2014;35 Suppl:S57-63.
32. Reiss K, Saftig P. The "a disintegrin and metalloprotease" (ADAM) family of sheddases: physiological and cellular functions. *Semin Cell Dev Biol*. 2009;20(2):126-37.
33. Moody SA. Fates of the blastomeres of the 16-cell stage *Xenopus* embryo. *Dev Biol*. 1987;119(2):560-78.
34. Luo T, Zhang Y, Khadka D, Rangarajan J, Cho KW, Sargent TD. Regulatory targets for transcription factor AP2 in *Xenopus* embryos. *Dev Growth Differ*. 2005;47(6):403-13.
35. Alfandari D, Wolfsberg TG, White JM, DeSimone DW. ADAM 13: a novel ADAM expressed in somitic mesoderm and neural crest cells during *Xenopus laevis* development. *Dev Biol*. 1997;182(2):314-30.
36. Heasman J, Kofron M, Wylie C. Beta-catenin signaling activity dissected in the early *Xenopus* embryo: a novel antisense approach. *Dev Biol*. 2000;222(1):124-34.
37. Sandelin A, Alkema W, Engstrom P, Wasserman WW, Lenhard B. JASPAR: an open-access database for eukaryotic transcription factor binding profiles. *Nucleic Acids Res*. 2004;32(Database issue):D91-4.
38. Bowes JB, Snyder KA, Segerdell E, Jarabek CJ, Azam K, Zorn AM, et al. Xenbase: gene expression and improved integration. *Nucleic Acids Res*. 2010;38(Database issue):D607-12.
39. Karpinka JB, Fortriede JD, Burns KA, James-Zorn C, Ponferrada VG, Lee J, et al. Xenbase, the *Xenopus* model organism database; new virtualized system, data types and genomes. *Nucleic Acids Res*. 2015;43(Database issue):D756-63.
40. Callery EM, Smith JC, Thomsen GH. The ARID domain protein drill1 is necessary for TGF(beta) signaling in *Xenopus* embryos. *Dev Biol*. 2005;278(2):542-59.
41. Ruff M, Leyme A, Le Cann F, Bonnier D, Le Seyec J, Chesnel F, et al. The Disintegrin and Metalloprotease ADAM12 Is Associated with TGF-beta-Induced Epithelial to Mesenchymal Transition. *PLoS One*. 2015;10(9):e0139179.

42. Gaultier A, Cousin H, Darribere T, Alfandari D. ADAM13 disintegrin and cysteine-rich domains bind to the second heparin-binding domain of fibronectin. *J Biol Chem.* 2002;277(26):23336-44.
43. Van Otterloo E, Li W, Bonde G, Day KM, Hsu MY, Cornell RA. Differentiation of zebrafish melanophores depends on transcription factors AP2 alpha and AP2 epsilon. *PLoS Genet.* 2010;6(9):e1001122.
44. Suzuki M, Okuyama S, Okamoto S, Shirasuna K, Nakajima T, Hachiya T, et al. A novel E2F binding protein with Myc-type HLH motif stimulates E2F-dependent transcription by forming a heterodimer. *Oncogene.* 1998;17(7):853-65.
45. Owens ND, Blitz IL, Lane MA, Patrushev I, Overton JD, Gilchrist MJ, et al. Measuring Absolute RNA Copy Numbers at High Temporal Resolution Reveals Transcriptome Kinetics in Development. *Cell Rep.* 2016;14(3):632-47.
46. Schmidt C, Kim D, Ippolito GC, Naqvi HR, Probst L, Mathur S, et al. Signalling of the BCR is regulated by a lipid rafts-localised transcription factor, Bright. *EMBO J.* 2009;28(6):711-24.
47. Prieur A, Nacerddine K, van Lohuizen M, Peeper DS. SUMOylation of DRIL1 directs its transcriptional activity towards leukocyte lineage-specific genes. *PLoS One.* 2009;4(5):e5542.
48. Abbruzzese G, Gorny AK, Kaufmann LT, Cousin H, Kleino I, Steinbeisser H, et al. The Wnt receptor Frizzled-4 modulates ADAM13 metalloprotease activity. *J Cell Sci.* 2015;128(6):1139-49.
49. Luo T, Matsuo-Takasaki M, Thomas ML, Weeks DL, Sargent TD. Transcription factor AP-2 is an essential and direct regulator of epidermal development in *Xenopus*. *Dev Biol.* 2002;245(1):136-44.
50. Deardorff MA, Tan C, Saint-Jeannet JP, Klein PS. A role for frizzled 3 in neural crest development. *Development.* 2001;128(19):3655-63.
51. Brouxhon SM, Kyrkanides S, Teng X, Athar M, Ghazizadeh S, Simon M, et al. Soluble E-cadherin: a critical oncogene modulating receptor tyrosine kinases, MAPK and PI3K/Akt/mTOR signaling. *Oncogene.* 2014;33(2):225-35.
52. Brouxhon SM, Kyrkanides S, Teng X, O'Banion MK, Clarke R, Byers S, et al. Soluble-E-cadherin activates HER and IAP family members in HER2+ and TNBC human breast cancers. *Mol Carcinog.* 2014;53(11):893-906.
53. Friedrich BM, Murray JL, Li G, Sheng J, Hodge TW, Rubin DH, et al. A functional role for ADAM10 in human immunodeficiency virus type-1 replication. *Retrovirology.* 2011;8:32.
54. Arima T, Enokida H, Kubo H, Kagara I, Matsuda R, Toki K, et al. Nuclear translocation of ADAM-10 contributes to the pathogenesis and progression of human prostate cancer. *Cancer Sci.* 2007;98(11):1720-6.
55. Hong CS, Devotta A, Lee YH, Park BY, Saint-Jeannet JP. Transcription factor AP2 epsilon (Tfap2e) regulates neural crest specification in *Xenopus*. *Dev Neurobiol.* 2014;74(9):894-906.
56. Su W, Xia J, Chen X, Xu M, Nie L, Chen N, et al. Ectopic expression of AP-2alpha transcription factor suppresses glioma progression. *Int J Clin Exp Pathol.* 2014;7(12):8666-74.
57. Li X, Glubrecht DD, Godbout R. AP2 transcription factor induces apoptosis in retinoblastoma cells. *Genes Chromosomes Cancer.* 2010;49(9):819-30.

58. Bennett KL, Romigh T, Eng C. AP-2alpha induces epigenetic silencing of tumor suppressive genes and microsatellite instability in head and neck squamous cell carcinoma. *PLoS One*. 2009;4(9):e6931.
59. Orso F, Fassetta M, Penna E, Solero A, De Filippo K, Sismondi P, et al. The AP-2alpha transcription factor regulates tumor cell migration and apoptosis. *Adv Exp Med Biol*. 2007;604:87-95.
60. Rhee C, Edwards M, Dang C, Harris J, Brown M, Kim J, et al. ARID3A is required for mammalian placenta development. *Dev Biol*. 2016.
61. Aghababaei M, Hogg K, Perdu S, Robinson WP, Beristain AG. ADAM12-directed ectodomain shedding of E-cadherin potentiates trophoblast fusion. *Cell Death Differ*. 2015;22(12):1970-84.
62. Rhee C, Lee BK, Beck S, Anjum A, Cook KR, Popowski M, et al. Arid3a is essential to execution of the first cell fate decision via direct embryonic and extraembryonic transcriptional regulation. *Genes Dev*. 2014;28(20):2219-32.
63. Aghababaei M, Perdu S, Irvine K, Beristain AG. A disintegrin and metalloproteinase 12 (ADAM12) localizes to invasive trophoblast, promotes cell invasion and directs column outgrowth in early placental development. *Mol Hum Reprod*. 2014;20(3):235-49.
64. Pudney M, Varma MG, Leake CJ. Establishment of a cell line (XTC-2) from the South African clawed toad, *Xenopus laevis*. *Experientia*. 1973;29(4):466-7.
65. Sato T, Sasai N, Sasai Y. Neural crest determination by co-activation of Pax3 and Zic1 genes in *Xenopus* ectoderm. *Development*. 2005;132(10):2355-63.
66. Rankin SA, Kormish J, Kofron M, Jegga A, Zorn AM. A gene regulatory network controlling hhex transcription in the anterior endoderm of the organizer. *Dev Biol*. 2011;351(2):297-310.
67. Cai H, Kratzschmar J, Alfandari D, Hunnicutt G, Blobel CP. Neural crest-specific and general expression of distinct metalloprotease-disintegrins in early *Xenopus laevis* development. *Dev Biol*. 1998;204(2):508-24.
68. Neuner R, Cousin H, McCusker C, Coyne M, Alfandari D. *Xenopus* ADAM19 is involved in neural, neural crest and muscle development. *Mech Dev*. 2009;126(3-4):240-55.
69. Cousin H, Gaultier A, Bleux C, Darribere T, Alfandari D. PACSIN2 is a regulator of the metalloprotease/disintegrin ADAM13. *Dev Biol*. 2000;227(1):197-210.
70. Livak KJ, Schmittgen TD. Analysis of relative gene expression data using real-time quantitative PCR and the  $2^{-\Delta\Delta C(T)}$  Method. *Methods*. 2001;25(4):402-8.
71. Tamura T, Cormier JH, Hebert DN. Characterization of early EDEM1 protein maturation events and their functional implications. *J Biol Chem*. 2011;286(28):24906-15.

## FIGURE LEGENDS:

**Figure 1: adam13 cleaves pcdh8l.** (A) Schematic representation of full length pcdh8l. A Flag tag (DYKDDDDK) was introduced just before the first cadherin repeat (EC1). The yellow arrow indicates the predicted cleavage site of adam13 based on the molecular weight of N- and C- terminal fragments. Red and blue asterisk indicate N and O glycosylation site respectively. The monoclonal antibody 2F4 was produced against the cytoplasmic domain (Red). (B) Western blot from transfected Hek293T cells. Glycoproteins from the conditioned media were purified on concanavalin-A agarose. The cleavage fragment was detected using the N-terminus Flag tag using the mAb M2. Total pcdh8l and adam13 were detected using mAb 2F4 and mAb 4A7, respectively. The Pro (P) and Metalloprotease (M) active forms of adam13 are indicated. (C) Histogram representing the percentage of embryos lacking fluorescent neural crest cell in the migration pathway. (D) Photographs of representative embryos with or without fluorescent migrating neural crest cells. Embryos were injected at the one-cell stage with a morpholino targeting adam13 (10 ng MO13). Messenger RNA for RFP alone or combined with the different constructs was injected at the 8-cell-stage in a dorsal animal blastomere. Each injection was compared to RFP injected in control embryos in which RFP positive cranial neural crest cells have successfully migrated into the branchial and hyoid arches (0% inhibition). N=number of embryos scored from three or more independent experiments. Error bars represent standard error to the mean. One-way ANOVA was performed to determine statistical significance. Statistically significant at \* $p < 0.05$ , \*\*\* $p < 0.005$ .

**Figure 1-Figure supplement 1: Characterization of mAb 2F4 to pcdh8l.** A) Western blot from total membrane extracted from 10 embryos at gastrula stage (Stage 10) and

early tailbud stage (Stage 20) detected using mAb2F4. B-C) Cranial neural crest explants on fibronectin. Explants were left to migrate for 5 hours and fixed in 1XMBS, 3.7% formaldehyde for 1 hour, permeabilized for 30 min in 1XMBS containing 0.5% TritonX100. Staining with mAb 2F4 (B) clearly shows a membrane staining while DAPI stains the nuclei (C). D) Wholemout immunostaining of tailbud stage embryo fixed in DENTS (20% DMSO 80% Methanol) using mAb 2F4. The red arrows indicate the tip of the cranial neural crest segments. The staining is identical to the one obtained by *in situ* hybridization with the *pcdh8l* probe. E) Western blot on Hek293T cells extract transfected with the various *Xenopus laevis* protocadherin. The mAb 2F4 only recognizes *pcdh8l* (PCNS).

**Figure 1-Figure supplement 2: adam13 overexpression increases *pcdh8l* fragments.**

Western blot with mAb 2F4 from glycoproteins isolated from 20 embryos at stage 20. The intact full-length *pcdh8l* protein (PCNS) is indicated as well as 2 main fragments (arrowhead 1 and 2). All 3 forms are detected in uninjected embryos (UI) but the fragments are increased in embryos overexpressing *adam13* (A13). The blot was re-probed with 15F, a polyclonal antibody directed against the *adam13* cytoplasmic domain (35). The Pro (P) and Mature (M) forms of *adam13* are indicated. Two exposures are provided to clearly detect the endogenous and overexpressed *adam13* protein.

**Figure 2: Adam13 knockdown reduces *pcdh8l* expression.** (A) Relative mRNA

expression of *pcdh8l* normalized to GAPDH obtained by real-time PCR. MO13 was injected at the one cell stage (10 ng) and embryos were collected at stage 20. Polyadenylated mRNA was extracted from non-injected and MO13 injected embryos (5 embryos each). (B) Representative images of whole mount *in situ* hybridization in which

MO13 (5ng) was injected in one of the two blastomeres and non-injected side serves as control. Image shows reduced mRNA levels of pcdh8l in MO13 injected side (star, 71% of 31 embryos). (C) Western blot on glycoproteins isolated from either control (Non Injected) or knock down (10 ng MO13) stage 20 embryos (25 embryos each). MO13 efficiently prevents the translation of adam13 (A13) as well as reduces the pcdh8l protein level. A monoclonal antibody to Xenopus Ribophorin 1 (Rpn1) was used as a loading control. Error bars represent standard error to the mean (Mean $\pm$  S.E.M). One-way ANOVA was performed to determine statistical significance. Statistically significant at \*p < 0.05

**Figure 2-Figure supplement 1: adam13 knockdown reduces pcdh8l expression in cranial neural crest (CNC) cells.** (A) Relative mRNA expression of pcdh8l normalized to GAPDH in isolated CNC explants. CNC explants (20) were dissected from either control embryos or embryos injected with MO13 (10 ng at 1-cell stage) at stage 17. (B) Western blot for pcdh8l and Rpn1 from CNC glycoproteins. Proteins were extracted from non-injected and MO13 injected CNC (20) and glycoproteins pulled down using Con-A-agarose beads. Western blot shows that MO13 at 10 ng reduces pcdh8l expression compared to non-injected. Error bars represent standard error to the mean (Mean $\pm$  S.E.M). One-way ANOVA was performed to determine statistical significance. Statistically significant at \*\*p < 0.01.

**Figure 3: Full-length adam13 induces pcdh8l expression in naïve ectoderm (animal cap cells).** One-cell stage embryos were injected with mRNA encoding various forms of adam13 (1 ng). Animal cap (AC) explants were dissected at stage 9 and grown in 0.5X MBS until sibling embryos reached stage 18 to 20. mRNA and protein was extracted

from AC for analysis of pcdh8l. (A) Quantitative real-time PCR from mRNA isolated from 10 animal caps. The relative level of pcdh8l expression was normalized to GAPDH. (B) Western blot for pcdh8l protein using mAb2F4. 30 AC were used to extract protein from embryos injected with various adam13 constructs. Western blot shows induction of pcdh8l by full-length adam13, whereas other constructs fails to induce pcdh8l expression. adam13 (A13), non proteolytic adam13 (A13E/A), adam13 lacking a cytoplasmic domain ( $\Delta$ Cyto), isolated adam13 cytoplasmic domain (GFP-C13). Error bars represent standard error to the mean (Mean $\pm$  S.E.M). One-way ANOVA was performed to determine statistical significance. Statistically significant at \*\*\*p < 0.001

**Figure 4. Adam13 knockdown reduces tfap2 $\alpha$  expression.** (A) Relative mRNA expression of AP2 $\alpha$  normalized to GAPDH (5 embryos). Real-time PCR analysis shows a 40% decrease in AP2 $\alpha$  expression in response to adam13 KD (B) Representative images of dorsal view of whole mount *in situ* hybridization with AP2 $\alpha$ . MO13 (5 ng) was injected in one of the two blastomeres (star). The non-injected side serves as control. adam13 KD reduces AP2 $\alpha$  expression in 76% of the embryos (N=29). (C) Luciferase activity of AP2 $\alpha$  promoter in cranial neural crest cells (CNC). One-cell stage embryos were injected with MO13 (10 ng). Control and KD embryos were further injected at the 8-cell stage with the AP2 $\alpha$ :luciferase reporter (100 pg) together with pRL-CMV (10 pg) in one animal dorsal blastomere. CNC explants were dissected from stage 15-17 embryos and individual explants were lysed to measure luciferase activity. The normalized values from 10 individual explants (two biological replicates) were used for each measure. Error bars represent standard error to the mean (Mean $\pm$  S.E.M). One-way ANOVA was



performed to determine statistical significance. Statistically significant at \* $p < 0.05$ , \*\* $p < 0.01$ .

**Figure 5: Adam13 induces pcdh8l via AP2 $\alpha$ .** (A, C, D) Relative expression of AP2 $\alpha$  and pcdh8l in naïve ectoderm (animal cap) by real-time PCR. One-cell stage embryos were injected with 1 ng of the various adam13 constructs and morpholinos and embryos were collected at stage 9 to dissect animal cap cells (AC). AC were grown in 0.5X MBS until sibling embryos reached stage 20 to 22. Messenger RNA was extracted from 10 AC for gene expression analysis. Expression was normalized using GAPDH and compared to the expression in non-injected AC (NI). (A) Real-time PCR data show that adam13 can induce AP2 $\alpha$  by more than 4 fold. Both proteolytic activity and the presence of the cytoplasmic domain are essential for full activation. (B) Luciferase activity of AP2 $\alpha$  promoter in Hek293T cells show induction by adam13 and ADAM19 but not ADAM9. For each transfection the Luciferase values were normalized to the Renilla values driven by the CMV promoter. In these assays, the absence of proteolytic activity (A13E/A) reduced AP2 $\alpha$  induction only slightly, while the deletion of the cytoplasmic domain ( $\Delta$ Cyto) prevented the activity. (C) Induction of AP2 $\alpha$  by adam13 was prevented by the KD of AP2 $\alpha$  (10 ng of MOAP2 $\alpha$ ) but not  $\beta$ -catenin (20 ng of Mo $\beta$ -catenin). (D) Expression of AP2 $\alpha$  in response of adam13 also depends on AP2 $\alpha$  but not  $\beta$ -catenin. Error bars represent standard error to the mean (Mean $\pm$  S.E.M). One-way ANOVA was performed to determine statistical significance. Statistically significant at \*\* $p < 0.01$ , \*\*\* $p < 0.001$ .

**Figure 6: adam13 binds to arid3a and foxd3.** (A) Co-immunoprecipitation of arid3a-flag with adam13. Arid3a-flag mRNA were injected in one cell stage embryos either alone or with the morpholino to adam13 (MO13.) Proteins were immunoprecipitated with a goat polyclonal antibody directed against the cytoplasmic domain of adam13 (g821, (24)) and blotted with M2 to detect the Flag-tag of arid3a. The flow through was used to detect arid3a. The immunoprecipitation were re-probed using 6615F to detect adam13 (35). (B) Co-immunoprecipitation of adam13 and FoxD3 from embryos. FoxD3-myc mRNA was injected at the one cell stage either alone or with MO13. Adam13 was immunoprecipitated using the goat polyclonal antibody to adam13 (g821), and the proteins were detected by western blot using either the myc antibody (9E10) or a rabbit antibody to adam13 (6615F). FoxD3 co-precipitated with endogenous adam13.

**Figure 7: adam13 requires arid3a for induction of AP2 $\alpha$ .** Relative expression of AP2 $\alpha$  (A) and pcdh8l (B) in animal caps from embryos injected with adam13 alone or with a morpholino to arid3a (20 ng) or FoxD3 (20 ng). Animal caps were extracted at stage 17.

**Figure 7-Figure supplement 1: adam13 does not induce arid3a and FoxD3 expression in Naïve ectoderm.** Animal caps were dissected from stage 9 embryos injected with the various constructs or morpholinos as indicated. RNA was extracted from AC at stage 20. Graphs show relative mRNA expression normalized to GAPDH for (A) arid3a and (B) FoxD3. Error bars represent standard error to the mean for three or more independent experiments. One-way ANOVA was performed to determine statistical significance. Statistically significant at \* $p < 0.05$ , \*\*\* $p < 0.005$ .

**Figure 8: adam13 induction of AP2 $\alpha$  and pcdh8l does not involve Smad2.** (A-B)

Relative expression of AP2 $\alpha$  and pcdh8l in animal caps dissected from control embryos, or embryos injected with adam13 or adam13 and a morpholino to Smad2 (MOSmad2, 25 ng). C) Luciferase assays in Hek293T cells show no induction of AP2 $\alpha$  promoter activity by Smad2 (0.5  $\mu$ g) or Smad 7 (0.5  $\mu$ g). Smad2 does not increase adam13 activation of the AP2 $\alpha$  promoter, while Smad7 does not reduce adam13 induction of AP2 $\alpha$  promoter. Smad2 and Smad7 were transfected with or without adam13 (0.5  $\mu$ g) along with AP2 $\alpha$  promoter-luciferase and the pRL-CMV (100 ng, 10 pg). The ratio of luciferase to renilla was used to normalize each transfection to the empty vector control (CS2). Error bars represent standard error to the mean (Mean $\pm$  S.E.M). One-way ANOVA was performed to determine statistical significance. Statistically significant at \*\*p < 0.01, \*\*\*p < 0.001.

**Figure 9: arid3a is critical for multiple gene expression in the CNC.** (A-C)

Representative dorsal view of neurula treated by whole mount *in situ* hybridization with probes for tfap2 $\alpha$  (AP2 $\alpha$ ), snai2 (Slug) and pcdh8l (PCNS). Eight-cell stage embryos were injected in one dorsal animal blastomere with the arid3a morpholino (5 ng, Asterisk). The percentage of embryos with reduced signal in the injected side is given in percentage. N is the total number of embryos obtained from each case. (D) Western blot using mAb2F4 to detect pcdh8l (PCNS). Glycoproteins from 25 embryos were extracted and purify on ConA-agarose beads. Rpn1 was used as a loading control . (E) Histogram representing the percentage of embryos lacking CNC migration. One-cell stage embryos were injected with MO13. Control or KD embryos were further injected at the 8-cell stage in one animal dorsal blastomere with mRNA for RFP, PCNS, AP2 $\alpha$  or Arid3a. Observation of the RFP fluorescence at stage 24-26 reveals that the inhibition of

migration by adam13 KD is partially rescued by pcdh8l and AP2 $\alpha$  but not Arid3a. Error bars represent standard error to the mean (Mean $\pm$  S.E.M). One-way ANOVA was performed to determine statistical significance. Statistically significant at \*p < 0.05, \*\*p < 0.01. (F) Representative examples of injected embryos. Posterior to the left, dorsal is up.

**Figure 10: adam13 regulates arid3a post-translational modification.**

Western blot from transfected Hek293T cells. (A-B) Cytoplasmic (C) and nuclear (N) extracts from cells transfected with the empty vector (CS2), Arid3a-flag, adam13 (A13) or both. The blots were re-probed with the transcription factor YY1 as a nuclear marker and GAPDH as a cytoplasmic marker. The full-length *Xenopus laevis* Arid3a is detected at approximately 60 kDa (Arid3a Long). A shorter fragment is detected at about 40 kDa (Arid3a Short). (A) Co-transfection of adam13 with Arid3a increases the Arid3a protein level in the cytoplasm by 30% and the shorter fragment of Arid3a in the nucleus by 5 folds. (B) Co-transfection of Arid3a with the proteolytically inactive mutant adam13 (A13E/A) or the mutant lacking the cytoplasmic domain (A13 $\Delta$ Cyto) does not increase the shorter fragment in the nucleus. (C) Membrane extract from Hek293T cells transfected with Arid3a-flag and the adam13 constructs. Co-transfection of Arid3a with adam13 increases the intensity of the 40 kDa Arid3a fragment. This is not observed in the absence of the adam13 cytoplasmic domain. In contrast, a much more significant increase is observed when Arid3a is co-transfected with the A13E/A mutant.

**Figure 11: Hypothetical model of adam13 function:** Adam13 at the membrane may associate with a cytoplasmic protease that cleaves Arid3a (1) to generate the short form

971 seen in figure 10. Arid3a is localized to lipid raft via its palmytoylation. Once adam13  
972 cleaves itself in the cysteine rich domain (2), gamma secretase cleaves the cytoplasmic  
973 domain od adam13 (3), releasing the complex that can translocate in the nucleus to  
974 activate tfap2 $\alpha$  transcription.

975

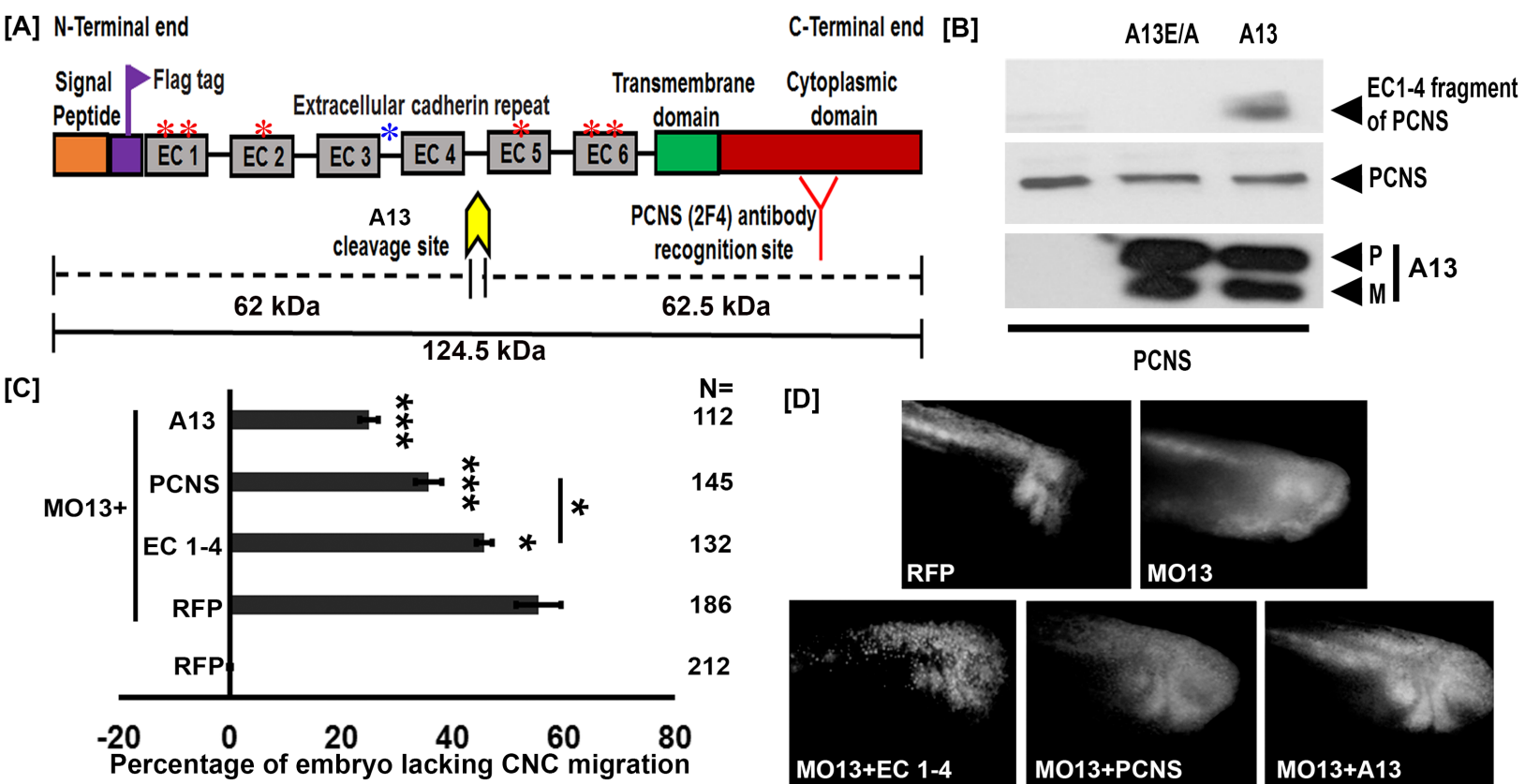
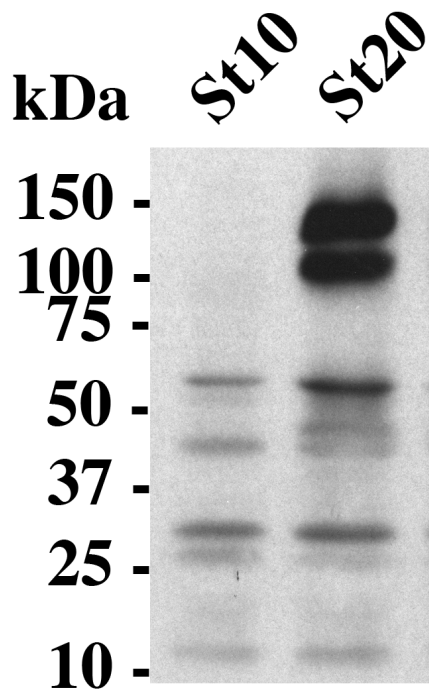
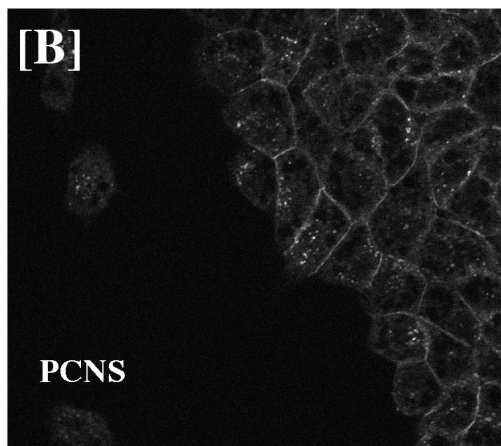


**Figure 1**

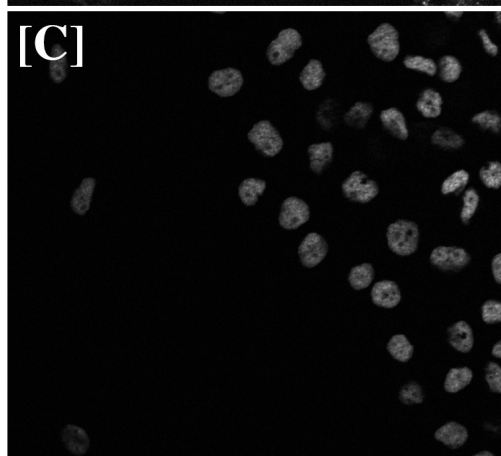
[A]



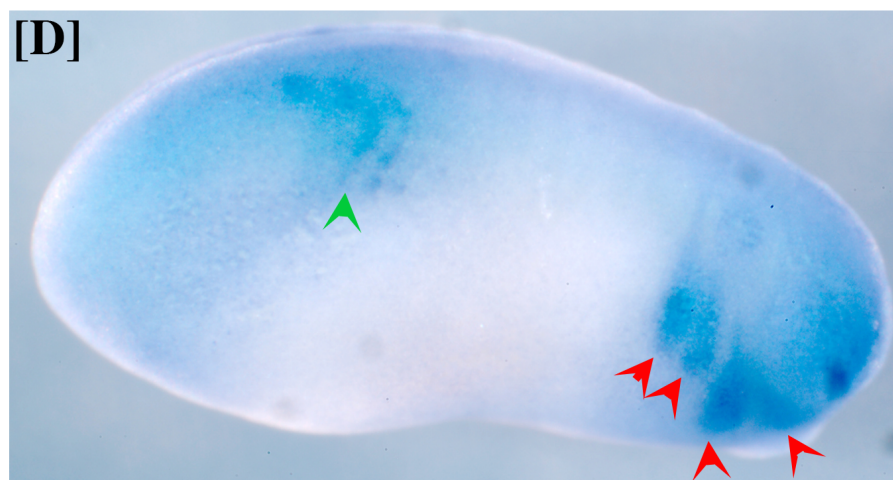
[B]



[C]



[D]



[E]

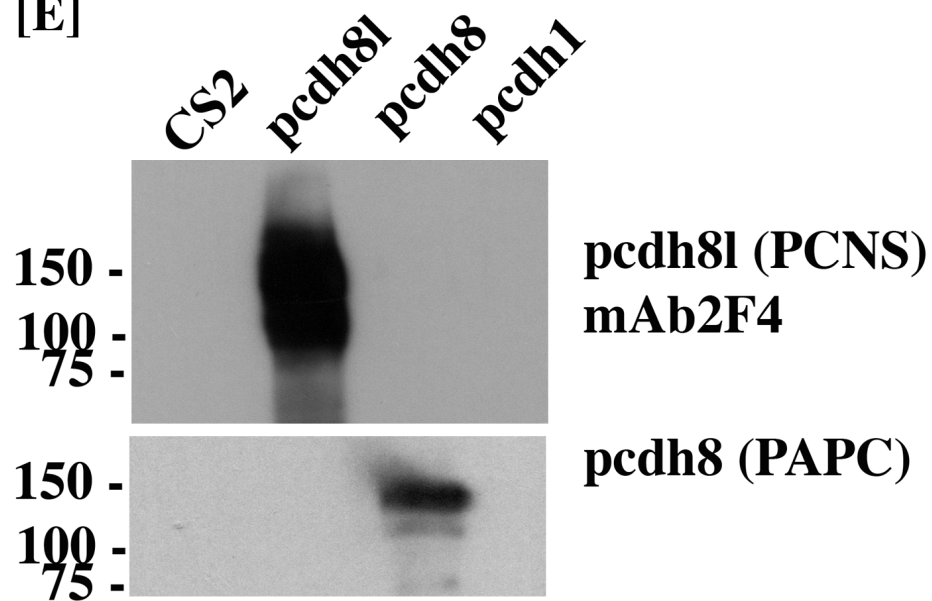


Figure 1:S1

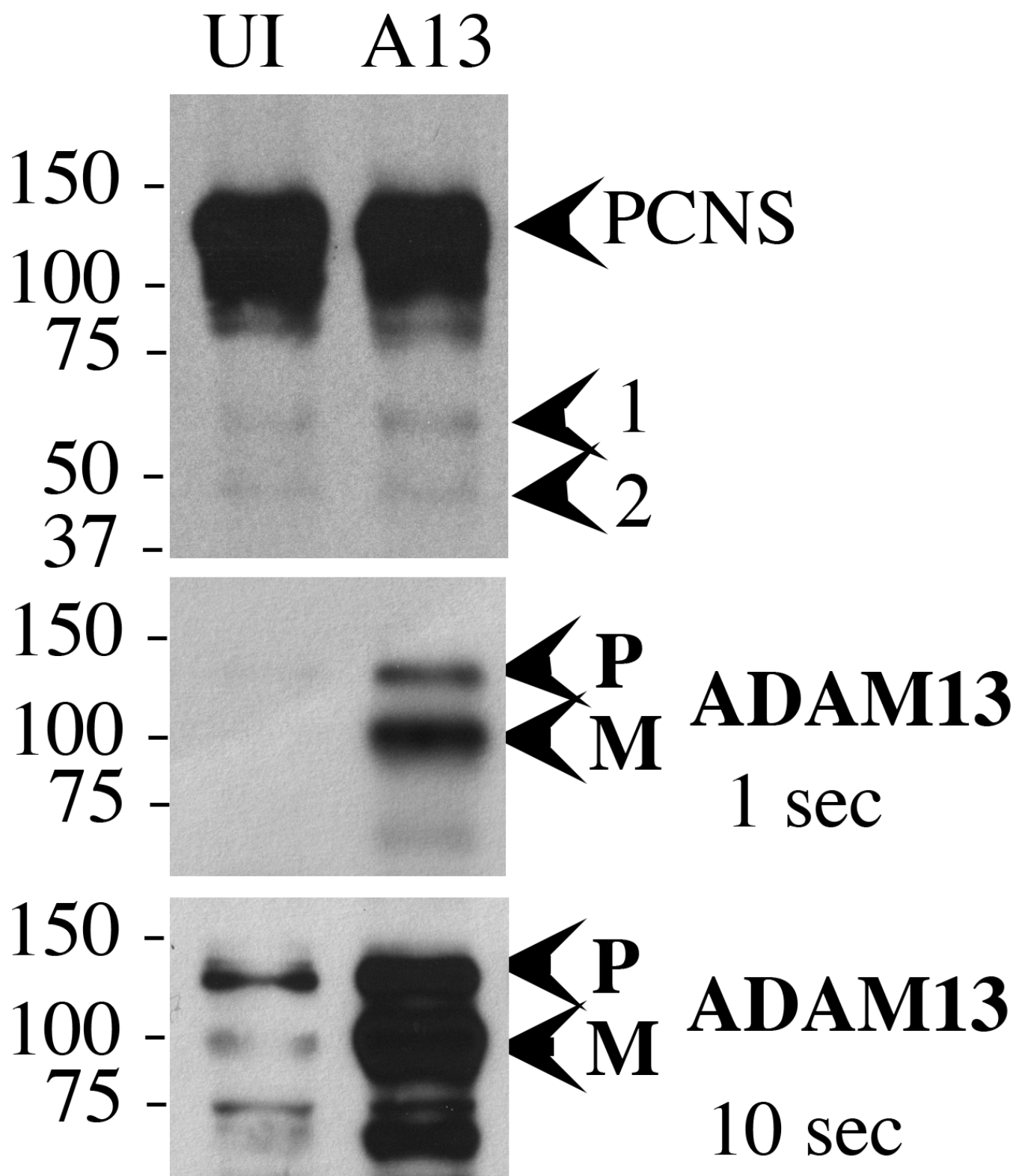
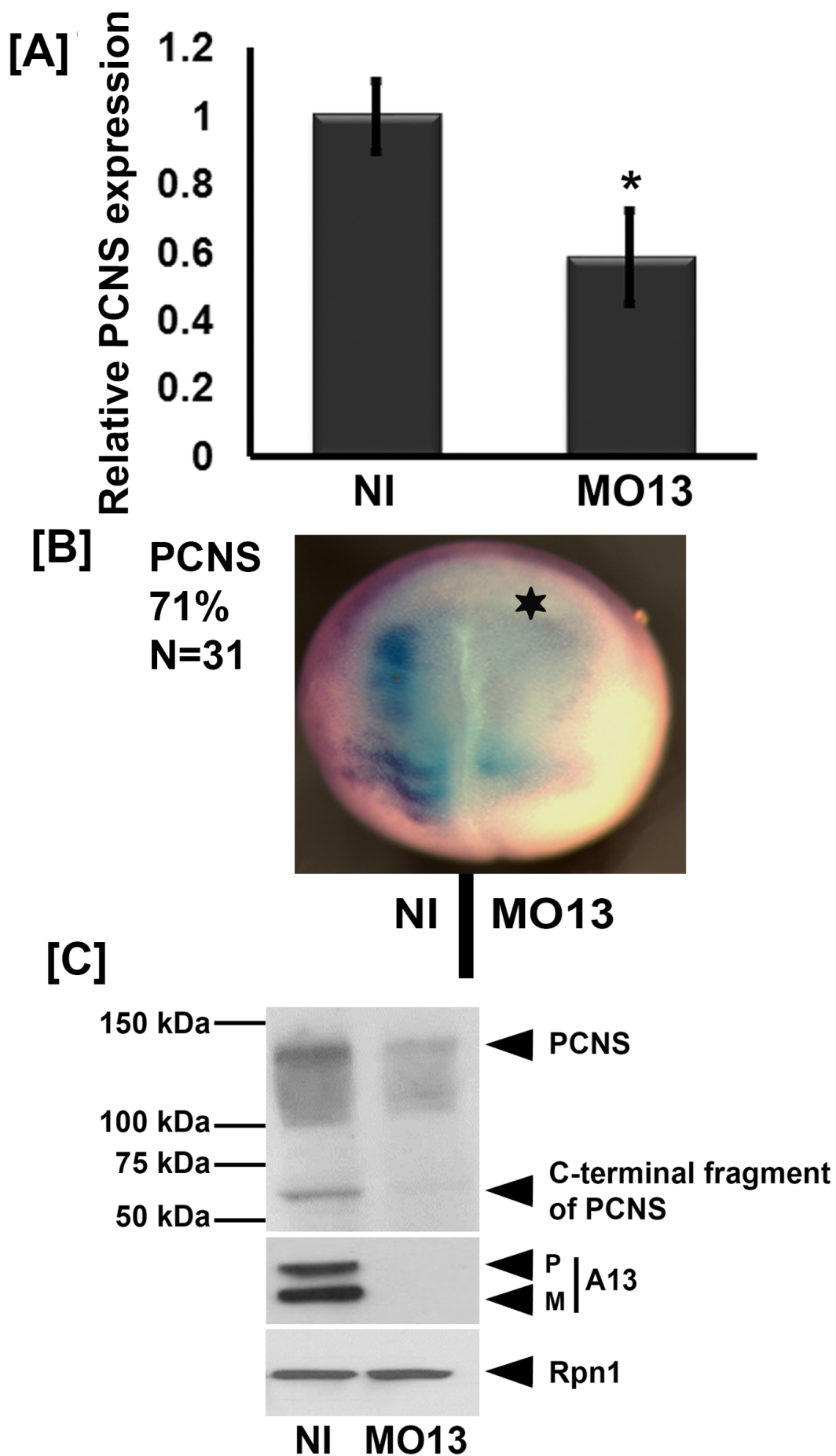
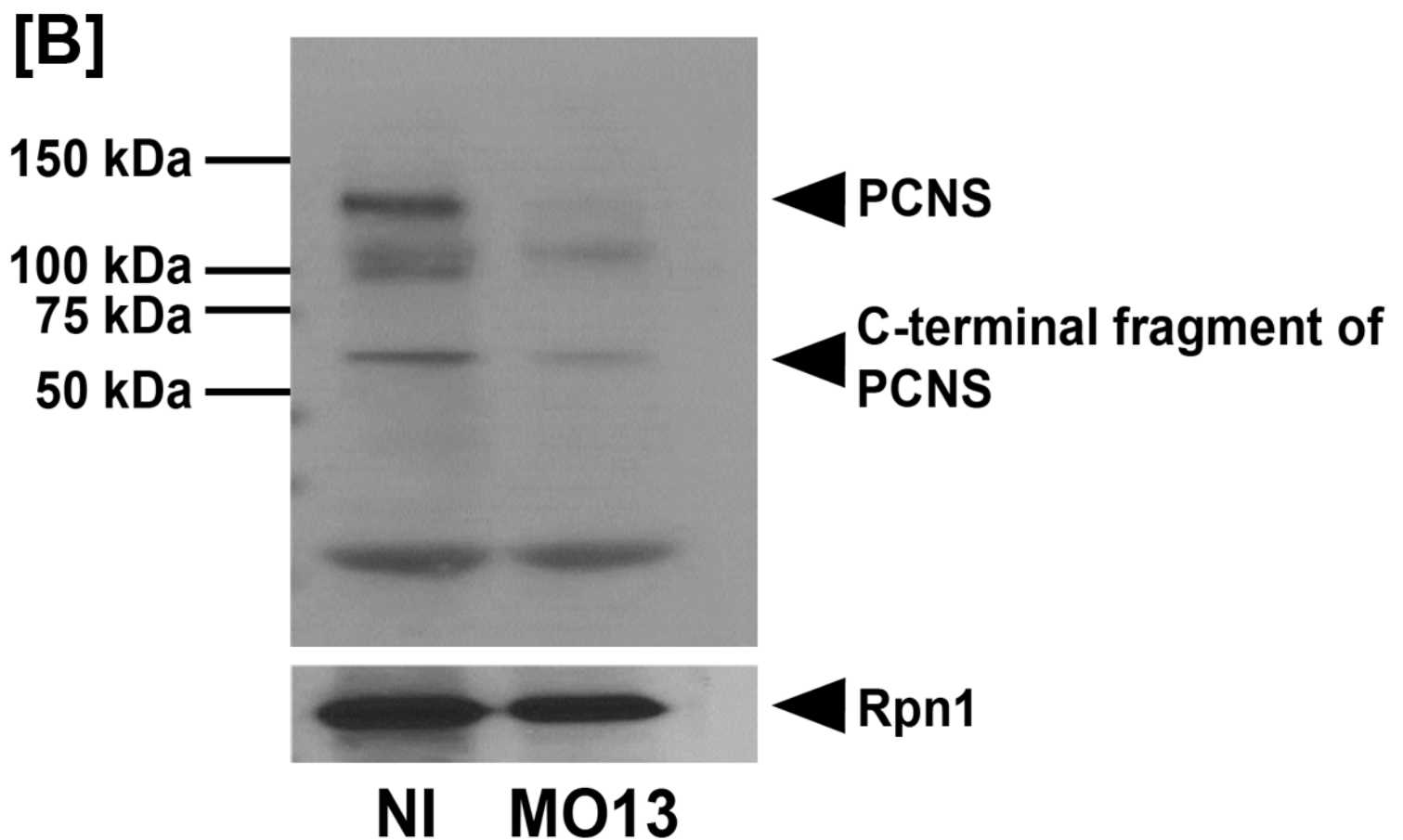
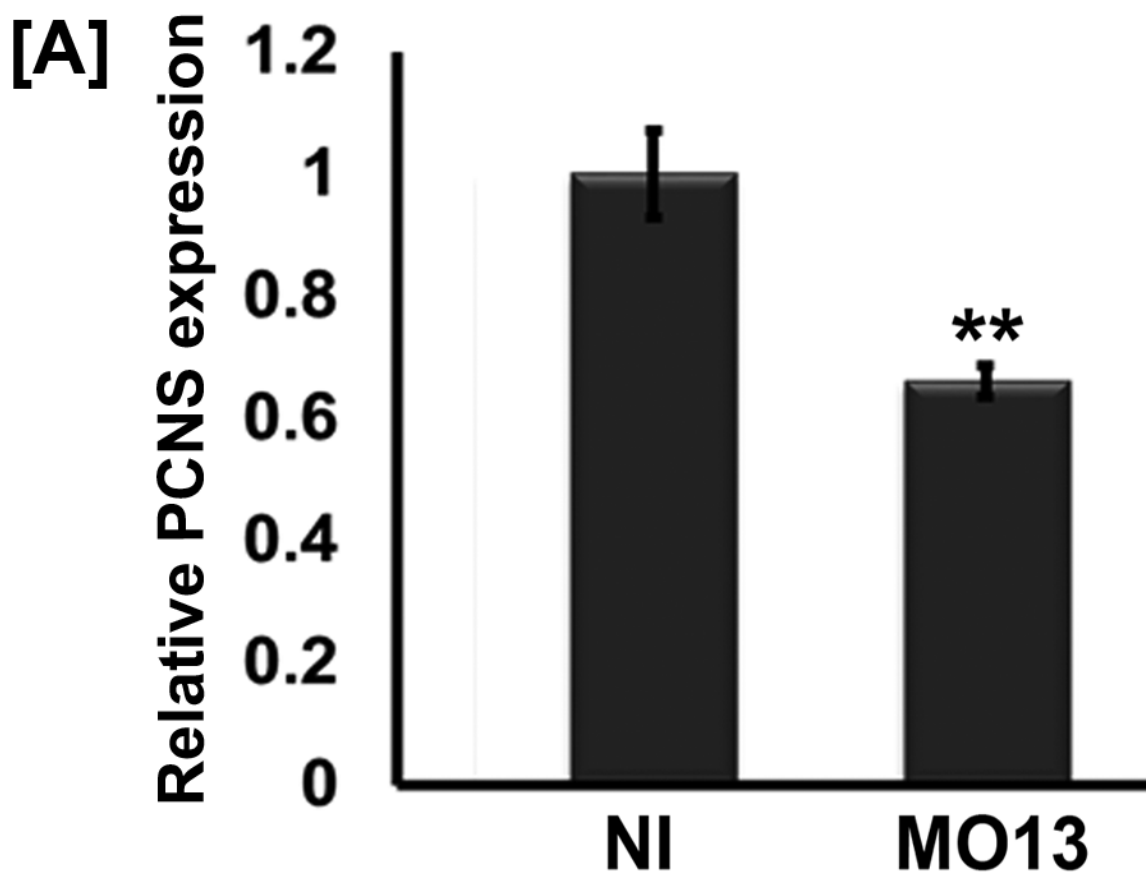


Figure 1:S2





**Figure 2**



**Figure2figure supplement 1**

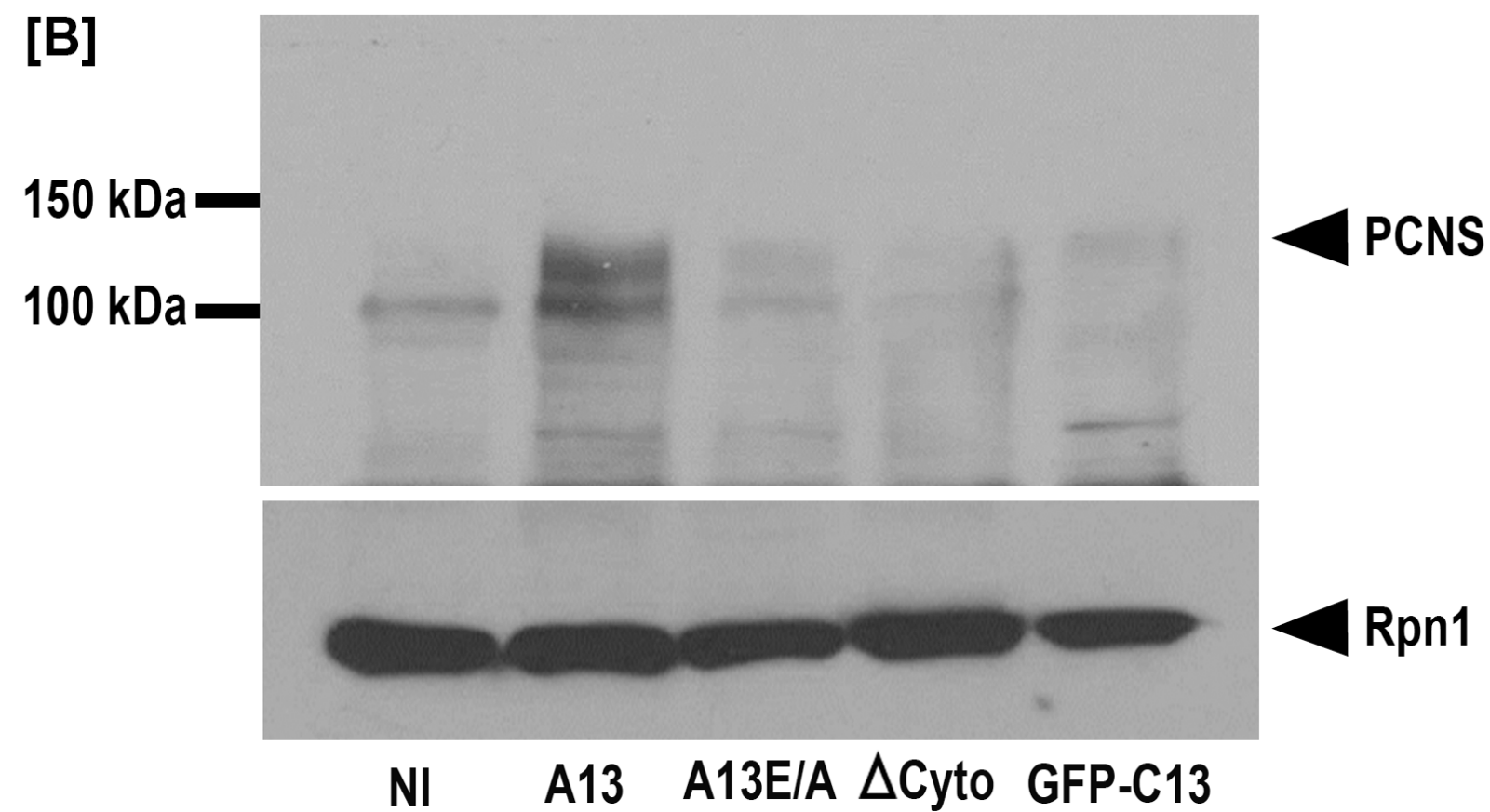
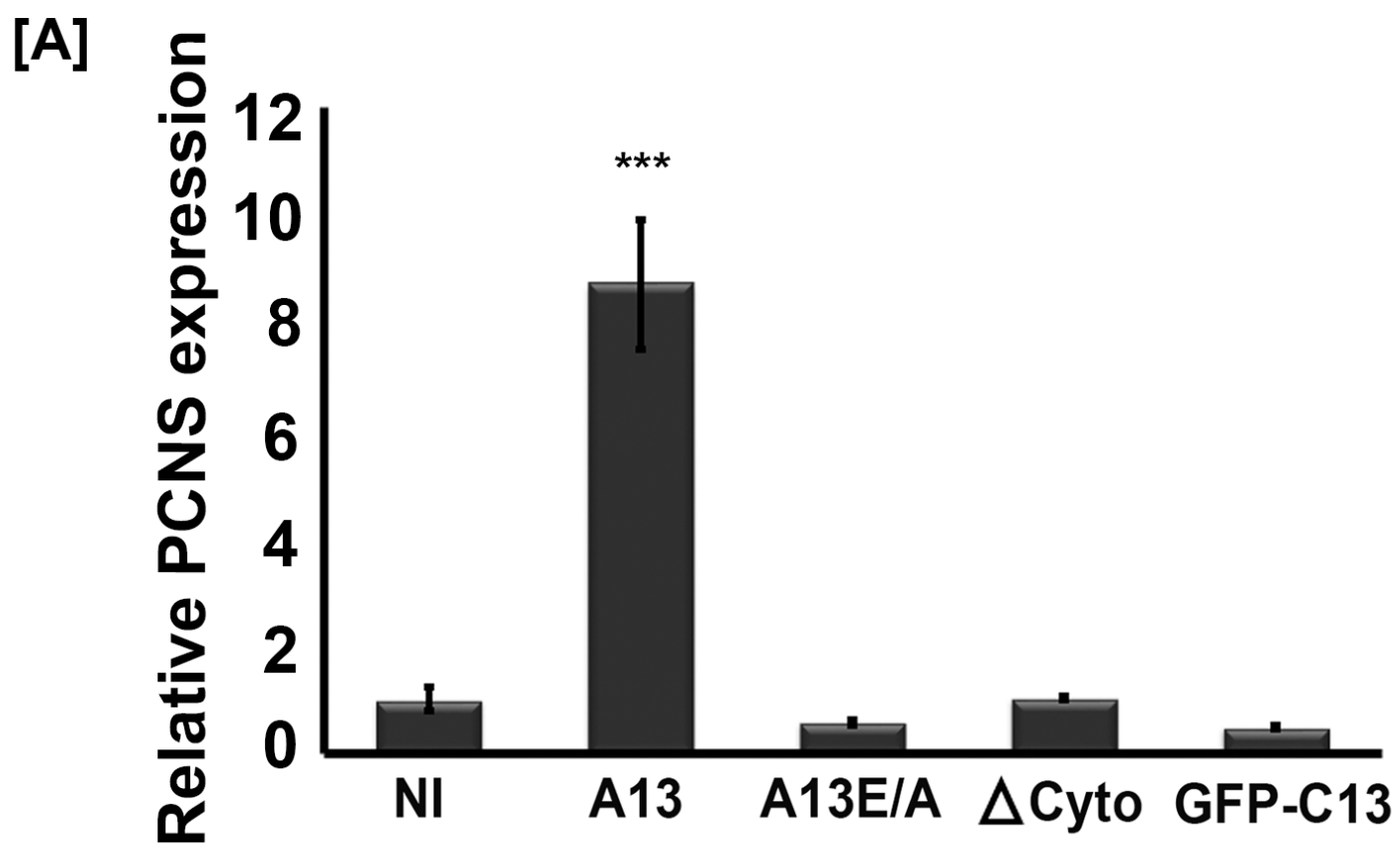


**Figure 3**

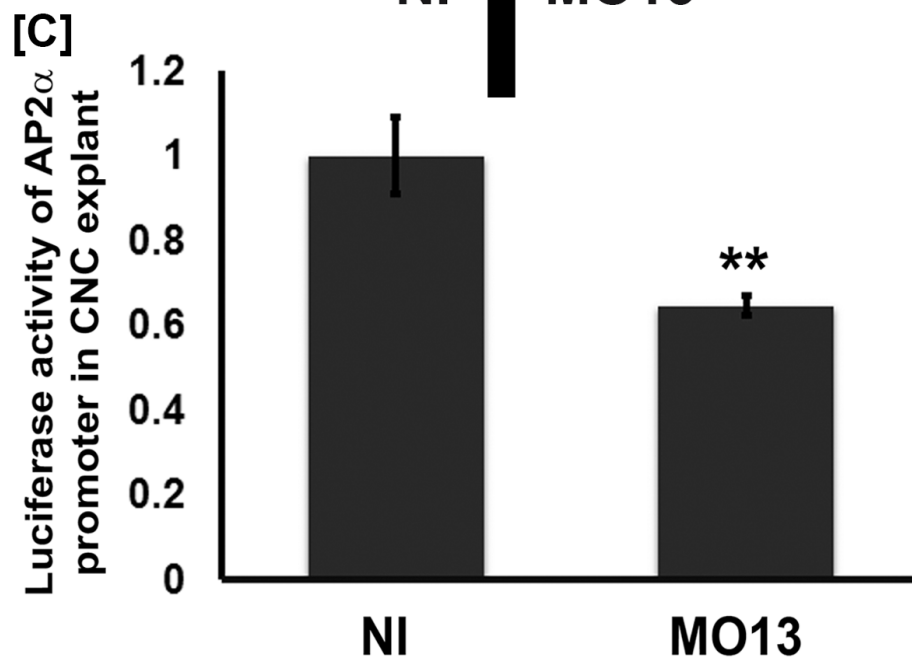
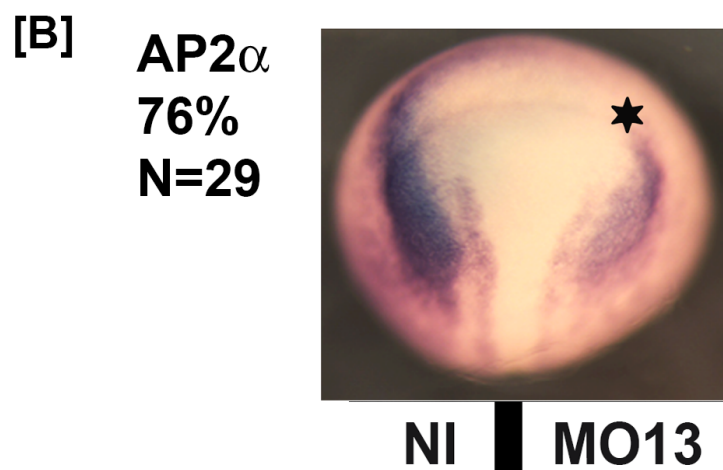
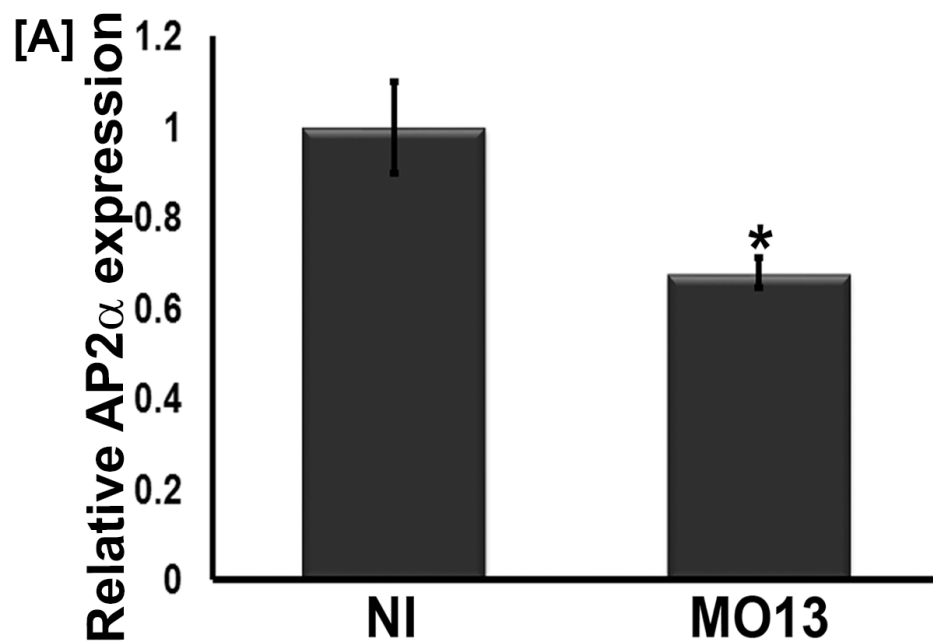


**Figure 4**

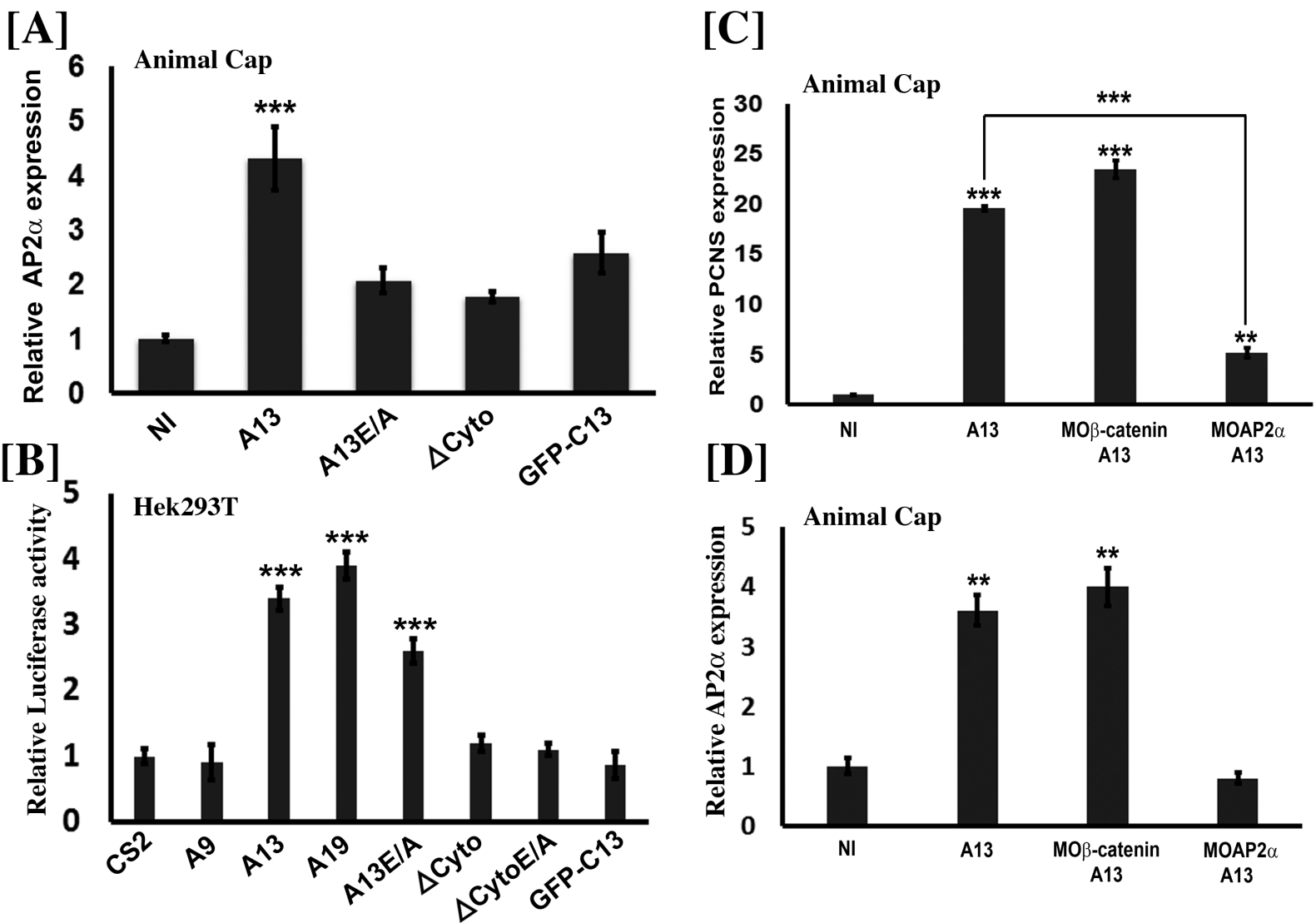
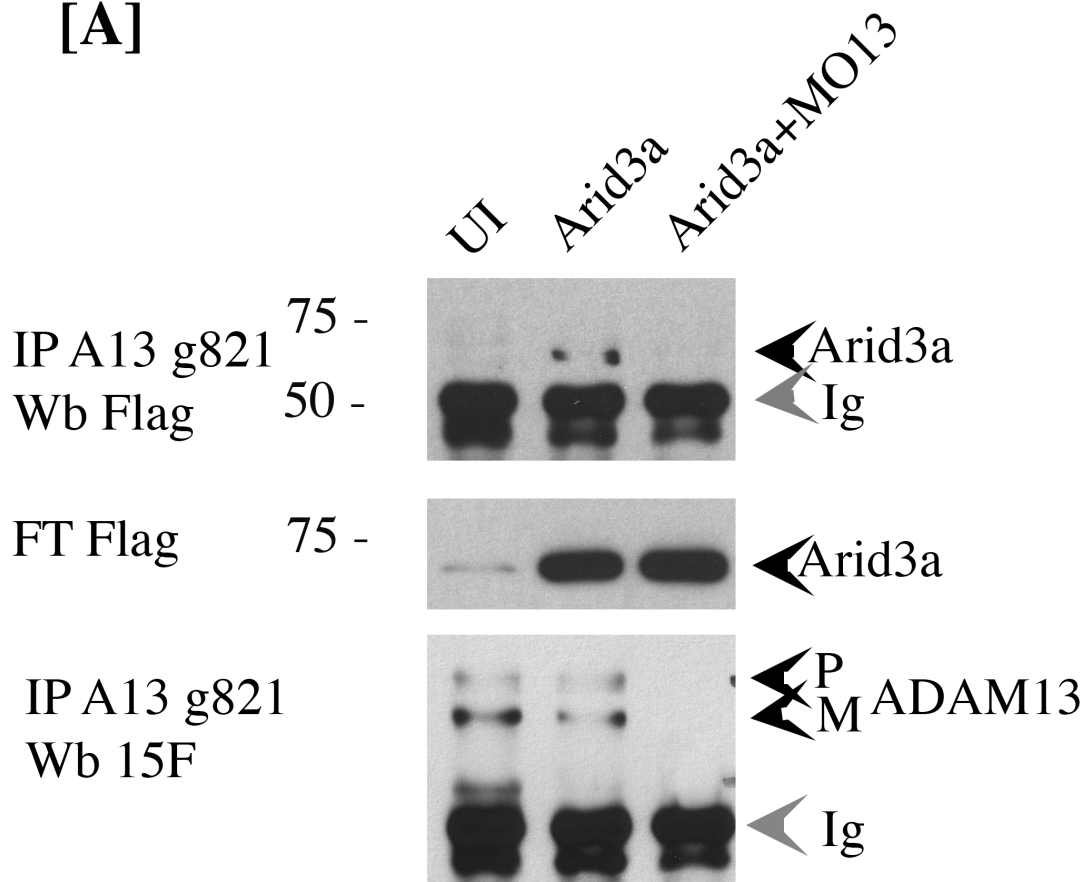


**Figure 5**

[A]



[B]

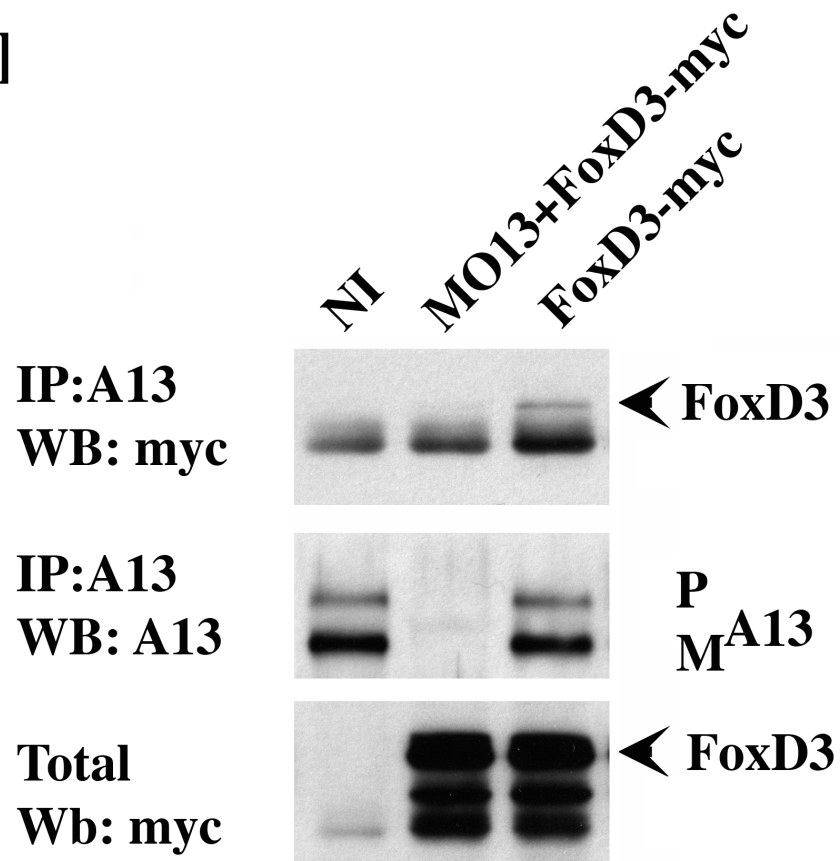
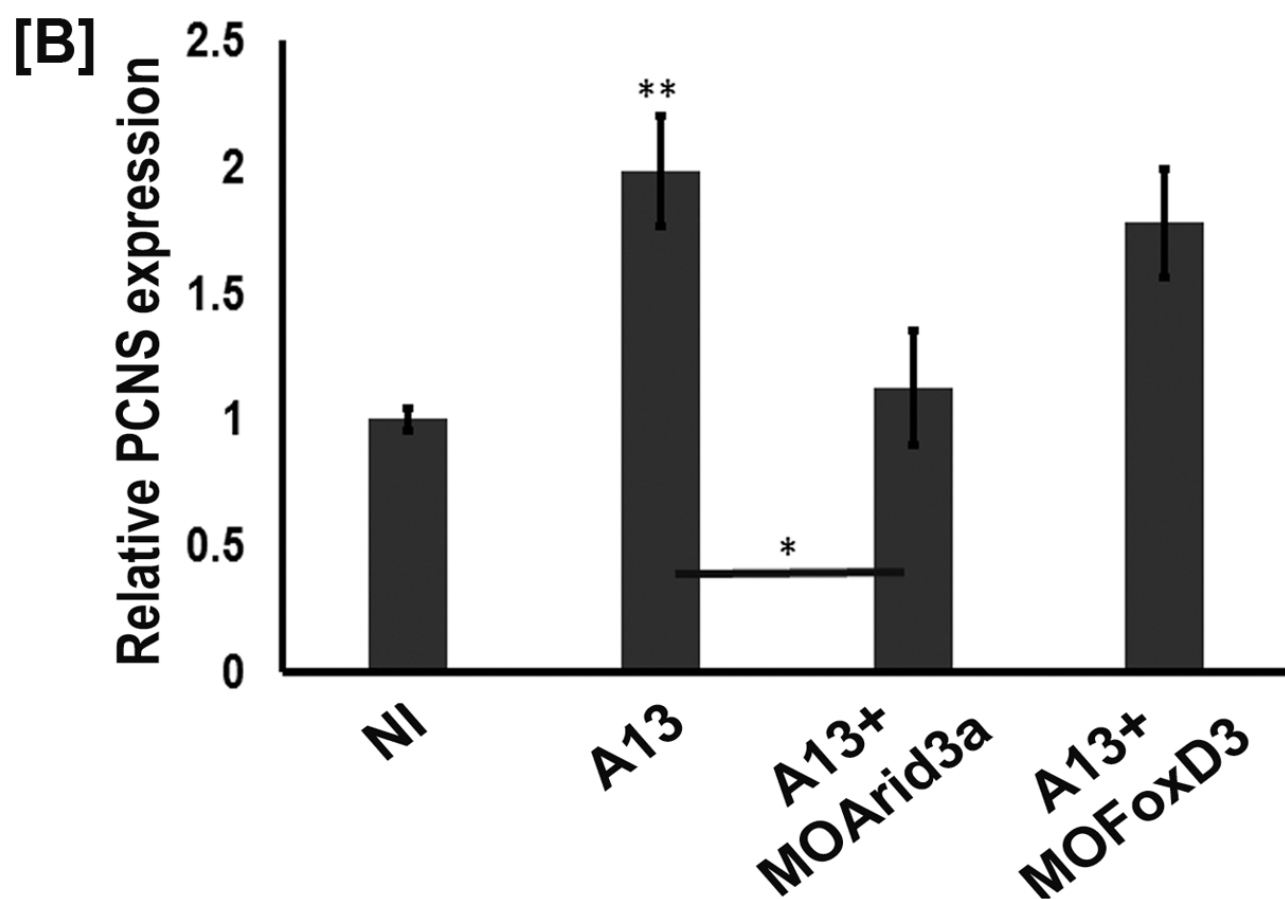
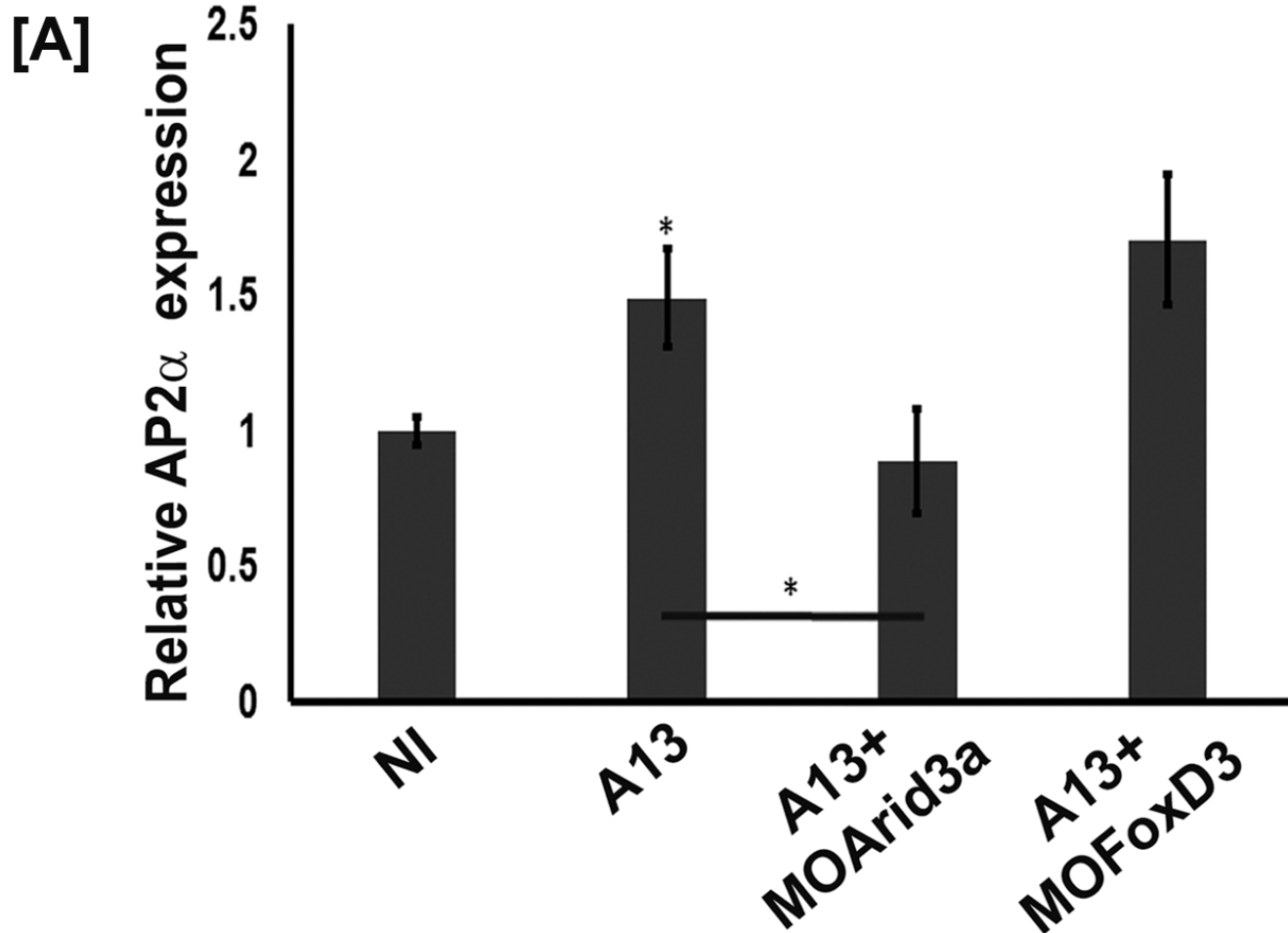
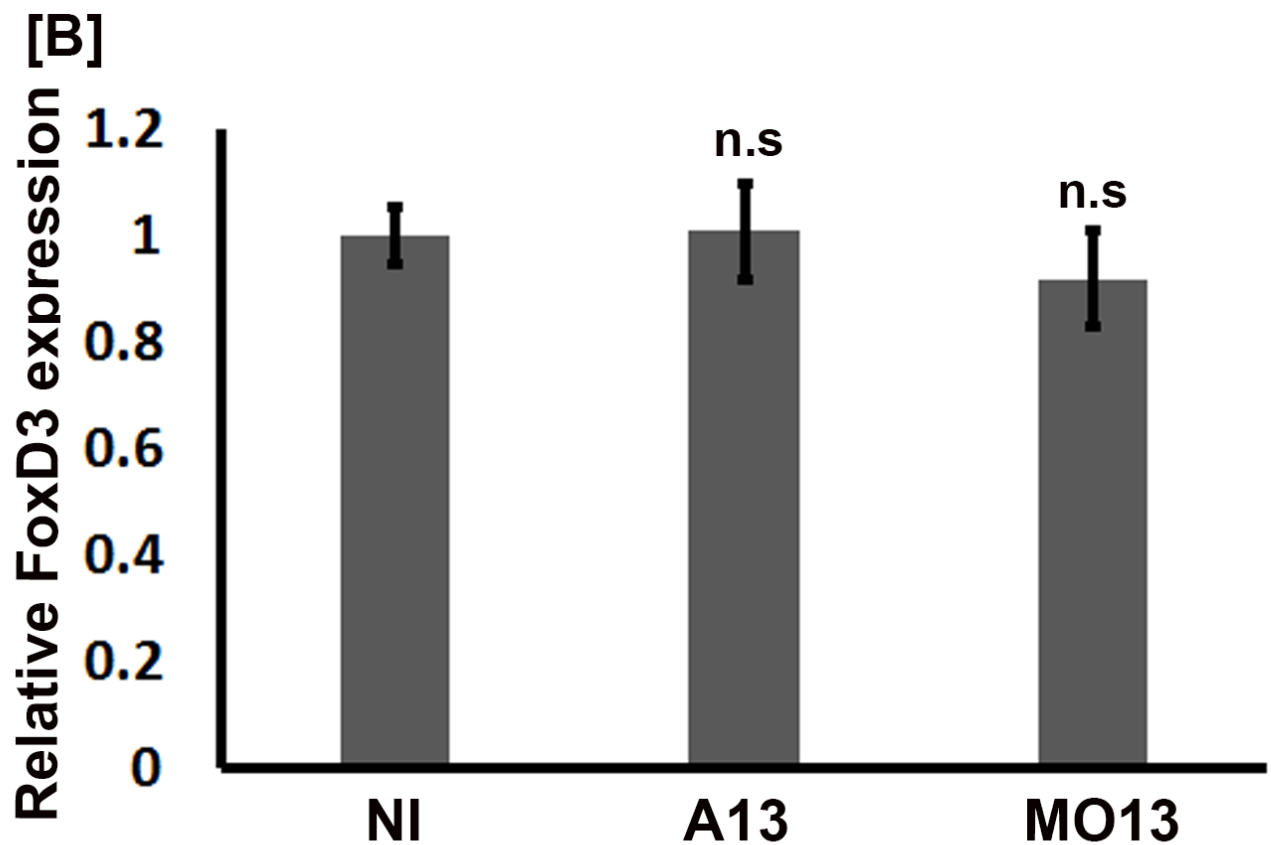
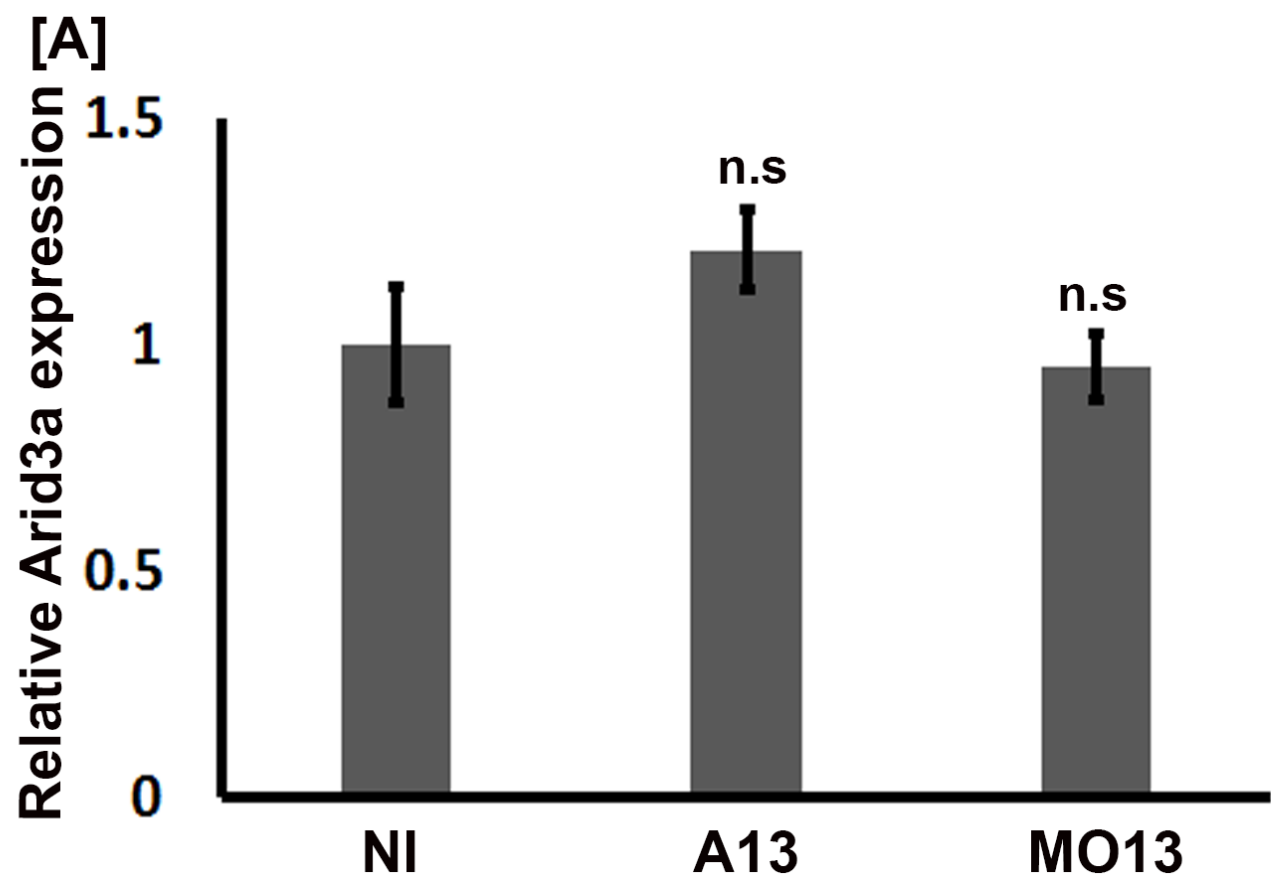


Figure 6



**Figure 7**



**Figure 7 figure supplement 1**



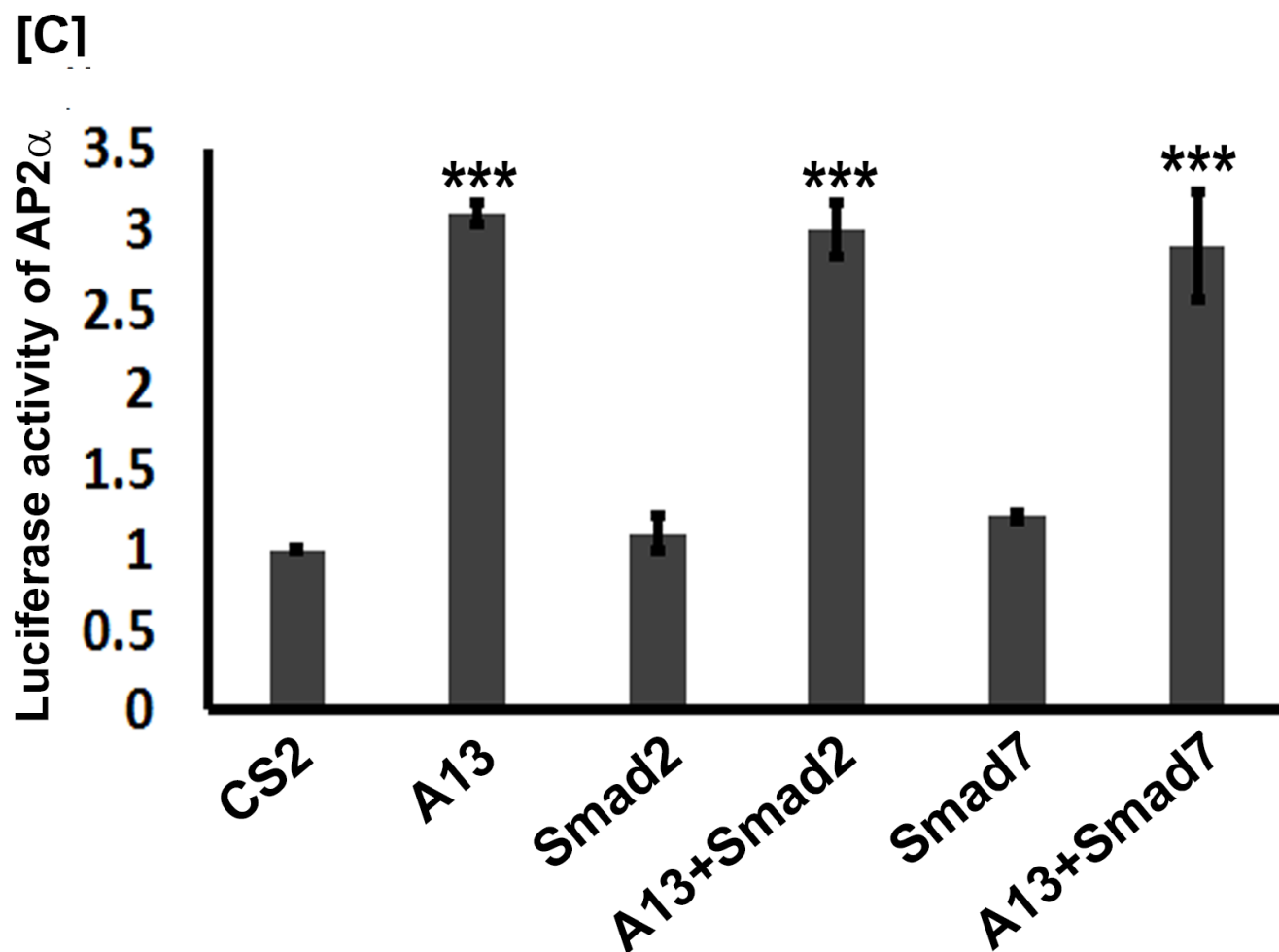
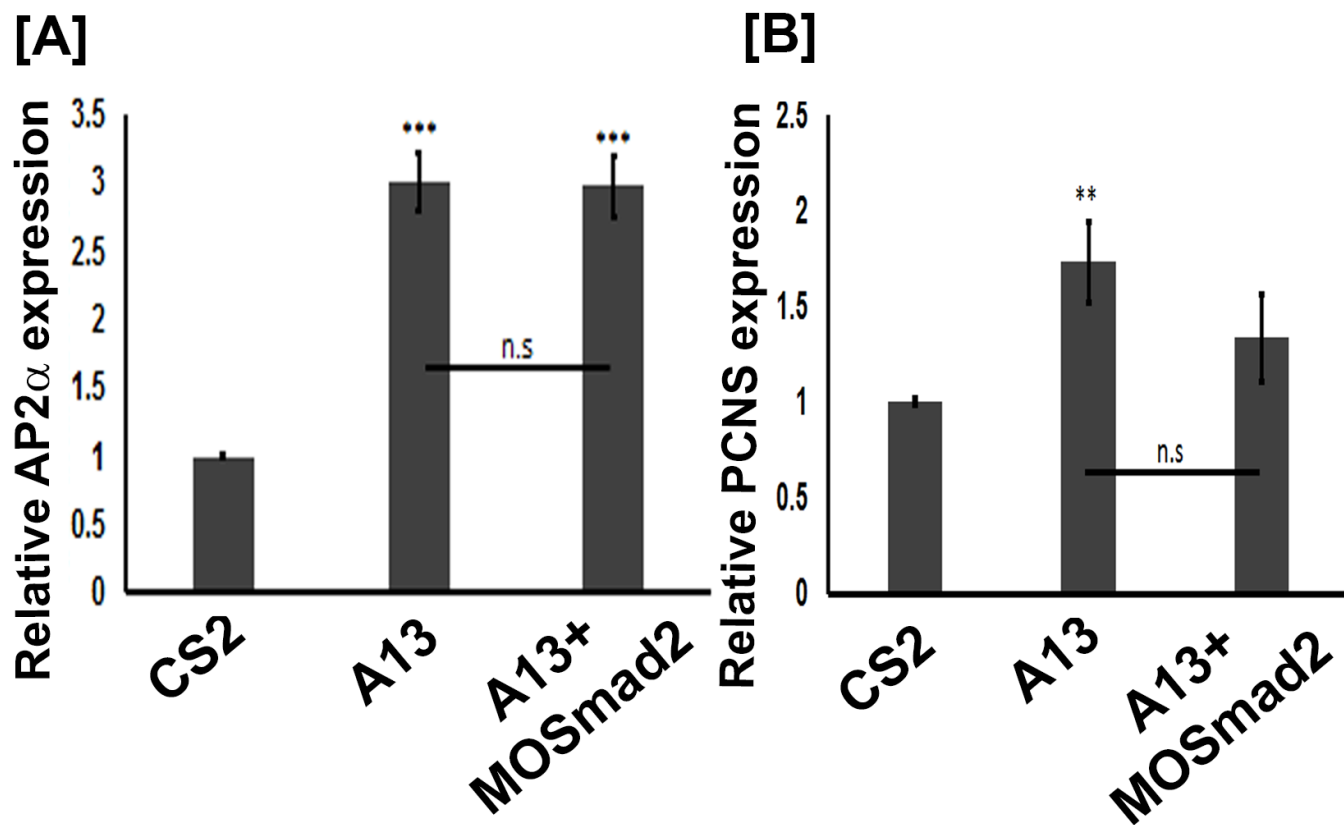


**Figure 8**

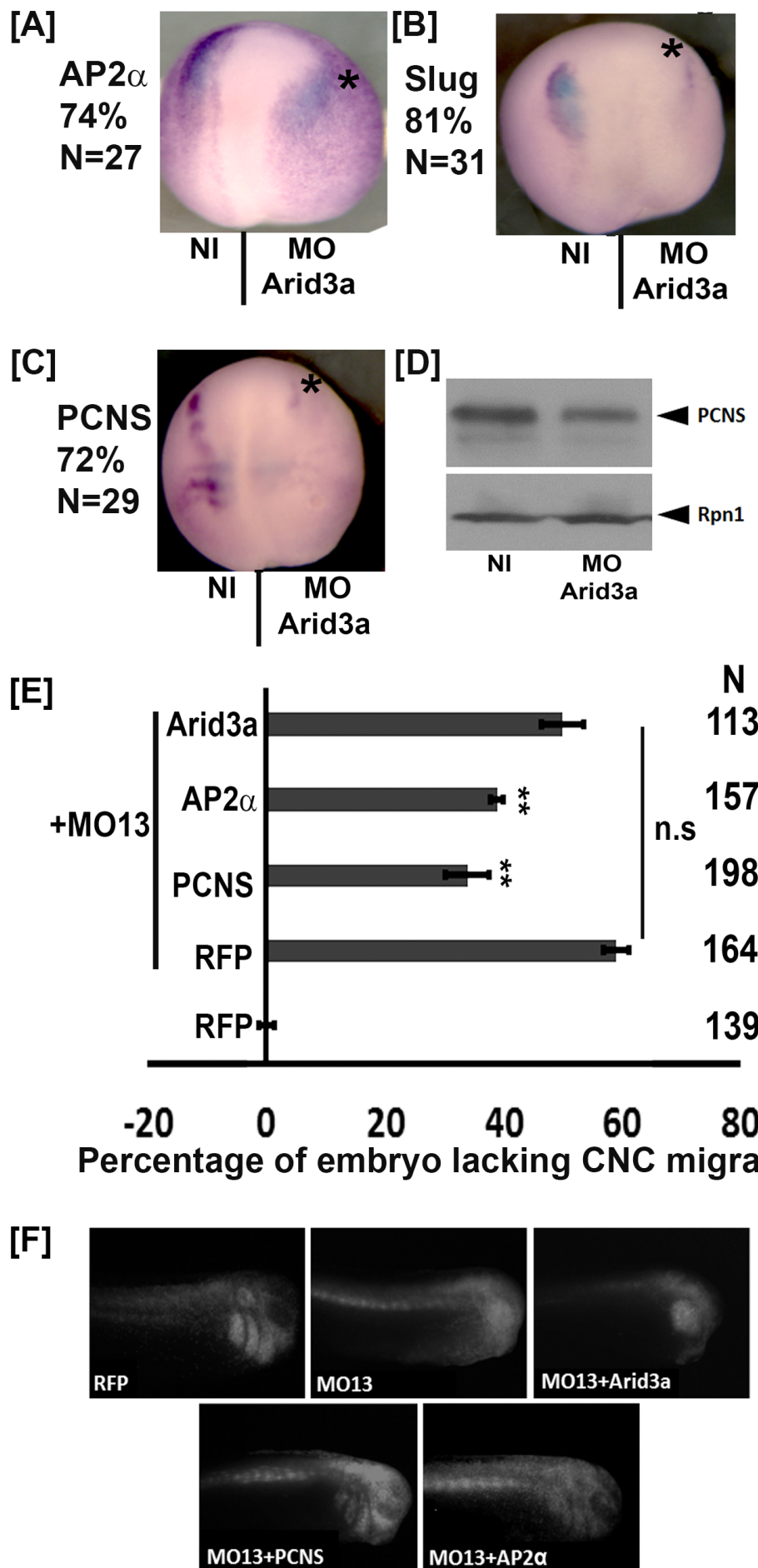
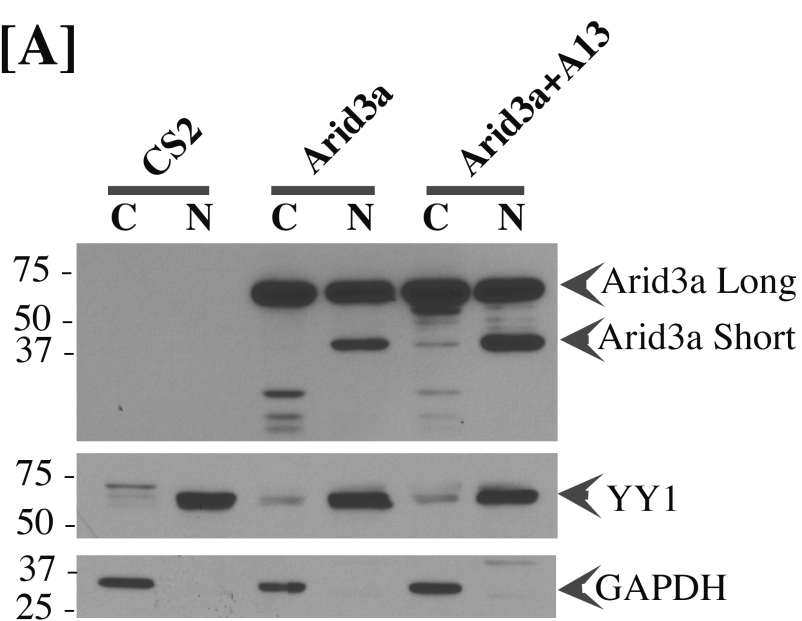
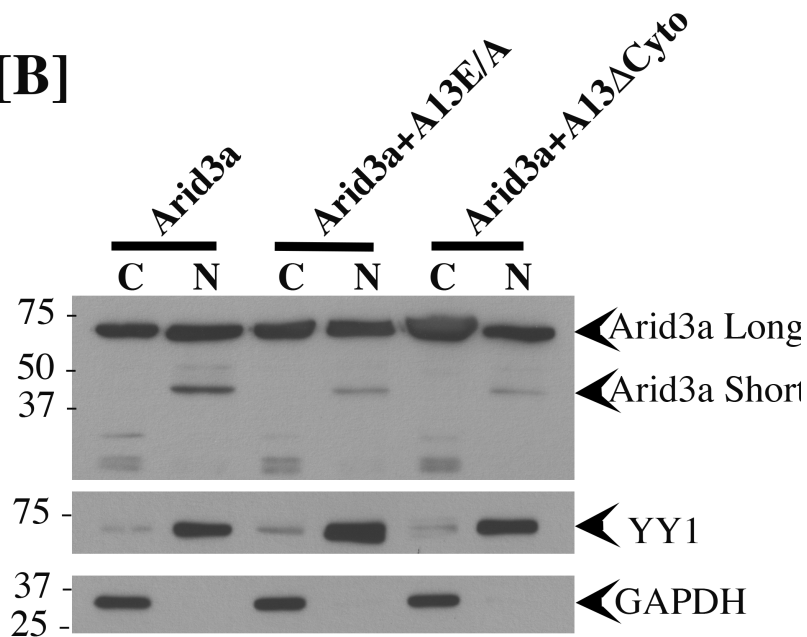


**Figure 9**

**[A]**



**[B]**



**[C]**

